JULIE KIÆR
SUPERVISOR: MALCOLM A. KELLAND

Design and Testing of Kinetic Hydrate Inhibitors

Master's Thesis 2024

Environmental Engineering

Department of Chemistry, Bioscience and Environmental Engineering

Faculty of Science and Technology

Abstract

The formation of gas hydrates, which restrict pipeline flow and delay oil and gas transport, is a challenge in the oil and gas industry. A chemical prevention method is the deployment of Kinetic Hydrate Inhibitors (KHIs) in the pipeline. KHIs delay hydrate formation and nucleation, allowing a safe operational window before hydrates start to form.

This thesis focuses on the synthesis of a brand new class of KHIs, polyvinyl amine oxides, and the testing of its KHI performance. There is an industrial need for commercially available alkylated amine oxides that can be synthesized in large quantities and have good KHI properties. Additionally, KHI performance tests are performed for the class poly(2-dialkylamino-2-oxazoline)s, received by the Hoogenboom group in Belgium.

The Slow Constant Cooling (SCC) method with high-pressure rocking cells was used as the primary performance test method. The test gas was Synthetic Natural Gas (SNG) or methane. Supplemental isothermal tests were carried out for the polyvinyl amine oxides.

The synthesis of the polyvinyl amine oxides showed that the polyvinyl dibutyl amine oxide ($PVAmBu_2O$) had the best KHI performance, likely resulting from the butyl groups and the amine oxide group. However, the synthesis needs refinement to obtain a reproducible product.

The SCC tests showed that some $PVAmBu_2O$ polymers performed better with increasing concentrations. Lower polymer molecular weight yielded the best performance. The addition of iBGE, nBGE, DPBGE and 3 wt.% NaCl improved the performance in SNG. Antagonistic effects by iBGE and nBGE were observed in the methane tests. A 2 °C onset temperature was obtained in the methane tests, indicating a potential for the polymer to be utilized in methane systems. In addition, the polymers outperformed PVCap in both test gases, indicating a new promising product that can be used in SNG and methane systems.

Isothermal tests revealed induction times of 2192 min (SNG) and 1068 min (methane) with a chemical blend of 5000 ppm $PVAmBu_2O$ and 5000 ppm nBGE. An unusual double pressure drop was observed in the SNG test.

The tests on the poly(2-dialkylamino-2-oxazoline)s showed similar performance to PVCap in SNG and methane. Synergism was obtained with iBGE, nBGE, DPBGE, and 3 wt.% NaCl while antagonistic effects were observed with TiPeAO and TiPeAB. In contrast, iBGE addition into the methane led to poorer performance.

Acknowledgments

First of all, I want to express my gratitude to my supervisor, Professor Malcolm Kelland, for his outstanding support and assistance throughout the laboratory work, particularly during the different syntheses, and for engaging in meaningful discussions about the lab results.

Secondly, I would like to thank PhD student Janronel Pomipic for teaching me how to operate the rocker rigs.

Thirdly, I want to thank my family for their support throughout all of my years of studying.

Last but not least, I would like to thank my greatest supporter, my boyfriend Johannes, for his invaluable support during this journey.

Table of Contents

1 Introduction

This chapter is dedicated to defining hydrates, how they form, the processes by which they plug the pipeline and the chemical means to control hydrate formation. The primary focus will be on KHIs and the performance assessment of their hydrate inhibition capacity. The last section of this chapter explains the main objectives of this thesis.

1.1 Background

A steady increase in the world`s energy consumption has been observed back to the 1950s [1]. Despite having green energy technology at hand, such as wind, tide, solar, and geothermal, the current level of technology fails to meet modern-day society`s energy demand, and thus, oil and gas production is still highly relevant [2].

One of the primary concerns in the oil and gas industry is ensuring flow assurance during production [3]. Flow assurance can be defined as the economical and efficient transportation of hydrocarbon fluids from the reservoir to the end user [4]. Relocating the drilling and production operations to ultra-deepwater areas (500 meters and below) results in flow assurance issues, where hydrate formation in the pipeline is one of the main concerns as it blocks the pipelines transporting oil and gas [5-7].

1.2 Hydrate Definition, Structure, Classification, and Formation

Gas hydrates are solid, clathrate (cage-like) structured compounds that consist of water molecules acting as a host lattice for various guest gas molecules such as methane, ethane, propane, hydrogen sulfide, and carbon dioxide. The host lattice structure of the hydrate contains spherical, asymmetrical cages of water molecules bound together by hydrogen bonds. The guest gas molecules within the cages are held in place by dispersion forces [8-10].

Hydrate formation requires the presence of four critical elements: low temperature (usually below 25 °C), high pressure (above 15 bars), water, and light hydrocarbon gases [6, 10].

The hydrate structure can be divided into three subcategories (**Figure 1.1**): structure I (sI), structure II (sII), and structure H. The difference in structure depends on the size of the guest gas molecule that can fit inside the water clathrate. Structure I hydrate can fit small gas molecules in the range of 0.4 to 0.55 nm, while structure II can host larger gas molecules with a size of 0.6-0.7 nm. Meanwhile, structure H can fit both sizes of guest gas molecules [11].

The cavities inside the hydrate structure vary in shape depending on the hydrate structure. Structure I forms a 14-sided cavity (also known as tetrakaidecahedron), which has a $5^{12}6^2$ configuration. This means the cavities consist of twelve pentagonal faces and two hexagonal faces. The guest molecules that occupy sI cages are small gas molecules such as methane, ethane, and carbon dioxide. Meanwhile, sII is slightly different from sI as it has 16 sides (hexakaidecahedral) and a $5^{12}6^4$ configuration with twelve pentagonal faces and four hexagonal faces. The guest gas molecules in this structure are also larger, such as propane and isobutane [8, 12].

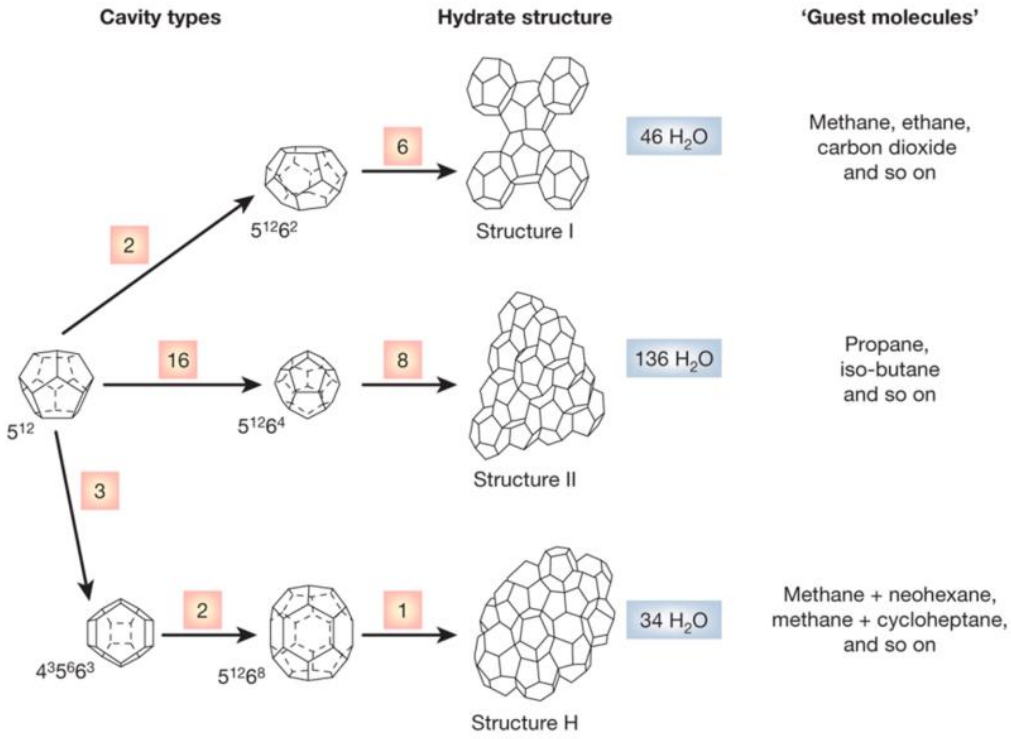

Figure 1.1 *Clathrate configuration, hydrate structure, and classification [12].*

Hydrates have physical properties that make them similar to ice, as their water content is around 85 mole percent. The density of the hydrate varies depending on the formation conditions and the guest gas molecules. A typical hydrate density is around 0.91 $\frac{g}{cm^3}$, meanwhile, water has a density of 1.0 $\frac{g}{cm^3}$ at 0 °C, respectively. This means that the hydrate will normally float at the interface between water and hydrocarbons [6, 13].

The formation of a hydrate crystal occurs in a two-step process which is called nucleation and growth. The first step, nucleation, involves the formation of several hydrate nuclei. Further growth of the nuclei occurs only after they have reached a critical radius [14]. The nucleation can be further divided into homogeneous nucleation and heterogeneous nucleation. The

homogeneous nucleation is stochastic, meaning that the critical nucleus is formed based on the system`s thermodynamic fluctuation. For this type of nucleation to occur, the nucleus must come from the parent phase, as this process does not rely on the presence of impurities. However, homogenous nucleation is difficult to achieve in the real world as it is believed that this can only be achieved when water droplets of high purity grade are dispersed in an oil emulsion. On the other hand, heterogeneous nucleation relies on the presence of impurities as the hydrate nuclei need to come in contact with a foreign surface or particle, lowering the interfacial energy required in the system. The growth of the nuclei cluster is achieved when a guest gas molecule residing in a water cluster adsorbs and diffuses over the surface of the growing crystal [8, 15].

1.3 Hydrate Formation and Dissociation Curve

Hydrate formation and dissociation curves (also known as hydrate stability curves) are important tools for gaining a better understanding of the hydrate behavior under different conditions of temperatures and pressures. The obtainment of these curves can be reached either by laboratory experiments or software using thermodynamic input [6]. The right side of the curve (**Figure 1.2**) represents an area of thermodynamic instability, whereas the left side represents an area of thermodynamic stability, where there is a formation potential as the hydrate is thermodynamically stable. Factors that affect the hydrate stability curve are oil, gas, water, and their different compositions. Hydrate formation requires that the system is subjected to a certain amount of subcooling. The term “subcooling” can be described as the difference between the actual operating temperature (at constant pressure) and the stability temperature of the hydrate [16]. An increase in subcooling is associated with a significant decrease in the hydrate formation time. The relationship between the two variables is exponential, where a higher subcooling leads to an exponential decrease in the hydrate formation time [6].

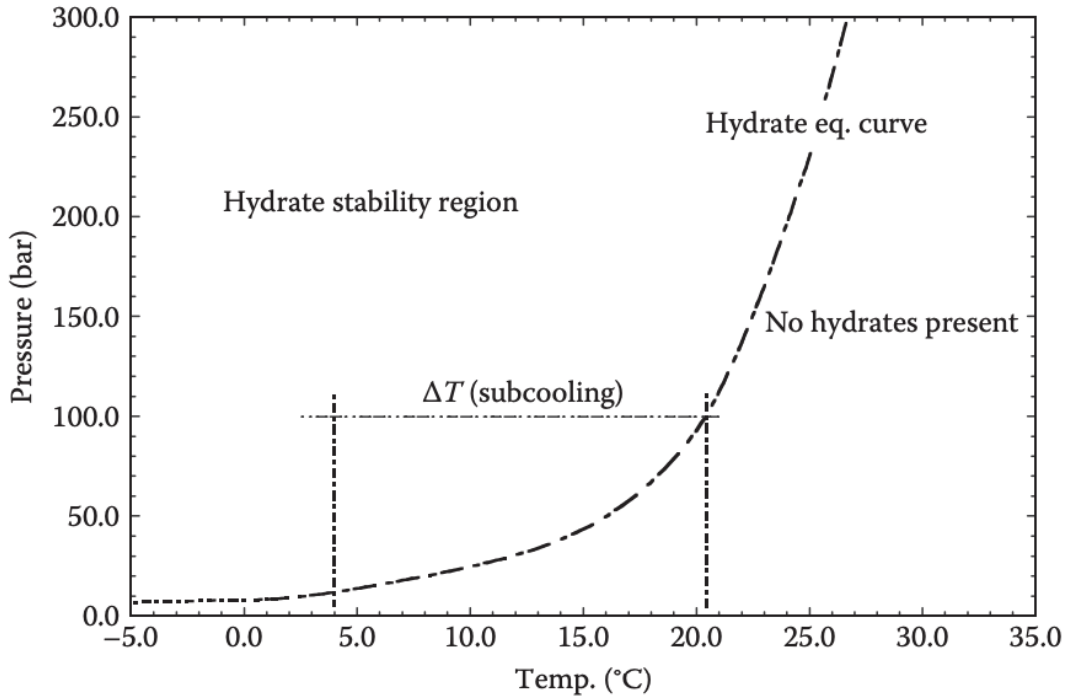

Figure 1.2 *Hydrate stability curve. The curve illustrates the pressure and temperature conditions where the hydrates are stable or unstable. On the left side of the curve, hydrates form and remain stable, while on the right side, no hydrates are present due to instability. This curve is a typical example of sII, natural gas hydrate stability curve [17].*

1.4 Hydrate Formation in the Pipeline

As previously mentioned, hydrate formation in the pipeline leads to an enormous flow assurance concern as the hydrates block the pipeline and restrict the flow of produced fluids. The formation of hydrates inside the pipeline (**Figure 1.3**) can be divided into four stages [18]:

Stage 1: Entrainment

Flow turbulence within the pipeline causes an emulsification of the oil, gas, and water phases. This leads to the formation of an oil-in-water emulsion, water-in-oil emulsion, or gas bubbles that are entrained in the oil and water phases.

Stage 2: Hydrate growth

As the temperature and pressures lie within the hydrate stability region, hydrate shells start to form around droplets consisting of water and oil that are emulsified in the oil/water phase. Further growth of the hydrate shells/particles is dependent on either mass transfer or heat

transfer. In the mass transfer case, the water or gas bubbles diffuse into the interphase between the oil and its respective phase.

Stage 3: Agglomeration

The hydrate particles start to assemble into larger clusters/aggregates. The interaction between the hydrate particles depends on the dominant aqueous phase in the pipeline system. Capillary bridging between the hydrate particles occurs if the system is oil-based. However, if the system is water-based, the particles remain dispersed due to weaker binding forces.

Stage 4: Plugging

Hydrate deposits on the pipeline wall lead to a narrower pipe annulus (orifice), which eventually causes complete pipeline blockage.

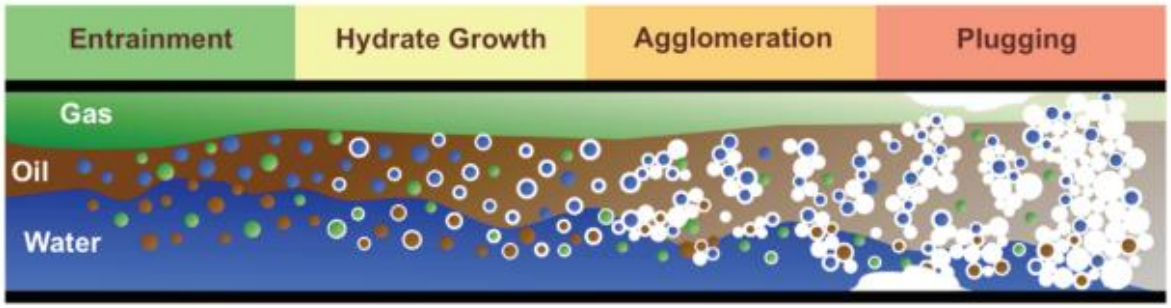

Figure 1.3 *Schematical representation of the different stages in pipeline plugging due to hydrate formation [18].*

1.5 Hydrate Plug Management with Inhibitory Chemicals

1.5.1 General Strategies

There are many ways to mitigate hydrate formation, and the management strategies can be divided into two subclasses: prevention and removal. On the prevention side, one can choose operational methods such as gas dehydration, pressure- and temperature control, or chemical methods such as Thermodynamic Hydrate Inhibitors (THIs) or Low-Dosage Hydrate Inhibitors (LDHIs). There is also an option of using non-chemical methods such as hydrate-repellent surfaces, ultrasonic methods, and biological methods. The removal of hydrates can also occur by chemical, non-chemical, and operational methods. Chemical methods include heat-generating chemicals and the use of THIs [19].

1.5.2 Thermodynamic Hydrate Inhibitors

Today, the most frequently used chemical method to address hydrate problems in the pipeline is the use of THIs. The THIs work by shifting the hydrate equilibrium curve into an area of even higher pressure and lower temperature, which means that the hydrate will not form until a low-temperature stage has been reached [6, 20]. Examples of THIs used in the field are alcohols, glycols, and salts. Among the classes of alcohols, methanol (CH_3OH) is the most well-known alcohol. A disadvantage of using methanol is that a large amount of it gets lost in the hydrocarbon phase, resulting in economic loss. A common glycol to mitigate hydrate inhibition is monoethylene glycol (MEG) ($HOCH_2CH_2OH$), which has a lower solubility in the gas phase and is easy to regenerate [19]. The advantages of using THIs are that they can melt an existing hydrate plug in the pipeline or prevent hydrates from forming [17].

There are several disadvantages when it comes to using THIs in the field. Perhaps the most important one is that they need to be added in doses as large as 20-60 weight percent to have an effect [20]. The large volumes required leads to increased capital expenditure (CAPEX) and operational expenditure (OPEX). Factors that contribute to a larger CAPEX are larger pumps that can handle such volumes, large storage tanks, and large regeneration facilities at the topside of the platform. Meanwhile, the OPEX increase is due to transportation, regeneration, and chemical procurement [3].

The use of conventional THIs are also problematic due to environmental concerns, as they pose a toxicity threat to humans and the environment [21]. Exposure of the aquatic environment to methanol has been found to cause a decrease in fish reproduction and subsequent growth. Fish subjected to lethal concentrations of methanol may experience issues with respiration and swimming. The lower trophic levels are also affected as crustacean plankton display a high methanol sensitivity in low concentrations, which may result in an altered functionality of the aquatic ecosystem where the food chain is affected [22].

1.5.3 Low Dosage Hydrate Inhibitors

The challenges that came along with using THIs led to the development of another class of hydrate inhibitors called low-dosage hydrate inhibitors [20]. LDHIs are typically categorized into Anti-Agglomerants (AAs) and KHIs. The LDHIs are referred to as low dosage because they require a low concentration dose (usually 0.1 to 1 weight percent) to work as a hydrate inhibitor compared to the high dose of THIs. The mechanisms of the two LDHIs are quite different: KHIs function as a hydrate delayer on the formation of hydrates and prevent

nucleation of the hydrate particles. The AAs, on the other hand, allow hydrates to form but stop the growth of the hydrate as they interfere with the agglomeration stage of the hydrate crystals, which results in a slurry of hydrate particles that are dispersed in the liquid hydrocarbon phase [23]. A visual representation of the effect of the various hydrate inhibitors inside the pipeline is provided in **Figure 1.4** [6].

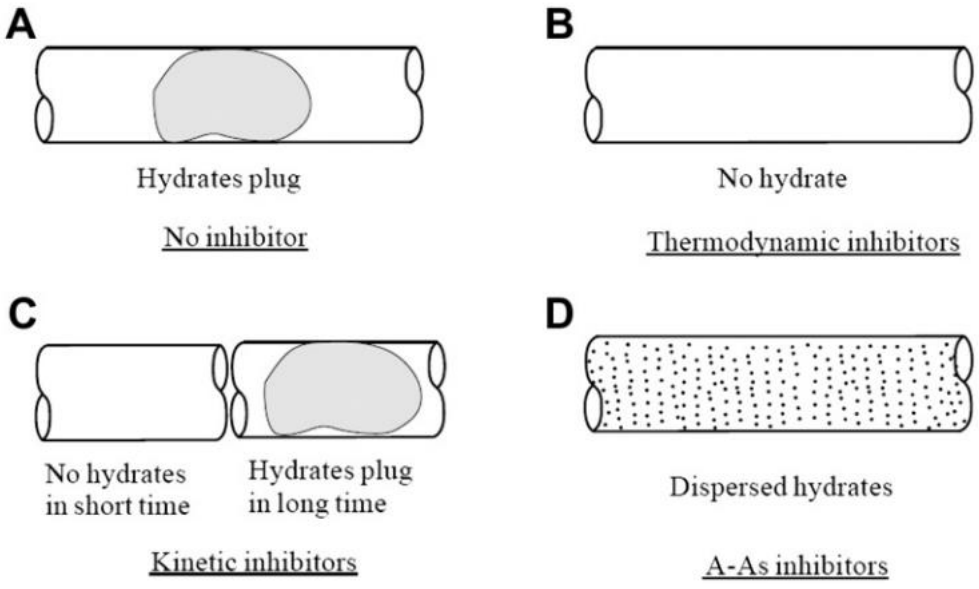

Figure 1.4 *Mechanism of various hydrate inhibitors' behavior inside pipelines [6].*

1.6 Kinetic Hydrate Inhibitors

The basis of commercial KHI formulations is to use water-soluble polymers. These water-soluble polymers can act alone on the hydrate or be paired with so-called synergists, which act as performance boosters. Two key components make up the polymers: a hydrogen-bonding functional group and a hydrophobic group. The hydrogen bonding functional group needs to be able to bind to the surface of the gas hydrate or onto the surface of the water molecules. Meanwhile, the hydrophobic group needs to be in direct contact with the hydrogen bonding functional group or lay adjacent to it [17].

The system's subcooling and pressure are the key factors that control the delay of the hydrate nucleation time and crystal growth. The delay time is commonly addressed in days as this allows for the safe transportation of production fluids from the well and into the processing facility without any risk of blocking the pipeline with a hydrate plug. Currently, KHIs can

produce a 9-10 °C subcooling. The subcooling can be thought of as the driving force for hydrate formation, and a higher subcooling would result in a shorter delay time [17].

1.6.1 KHI Classification

Commercial KHIs can be divided into three main categories: poly(N-vinyl lactam) polymers, hyperbranched polyesteramides, and isopropylmethacrylamide polymers [24].

1.6.1.1 Poly(N-vinyl lactam) polymers

A common structure identity with this KHI class is the lactam ring [24]. The lactam ring can be of different sizes, and studies have suggested that an increased ring number leads to increased KHI performance. The suggested mechanism is correlated to the cloud point of the polymer [17]. The cloud point can be defined as the temperature where a phase separation of the polymer occurs due to a temperature increase, which leads to a turbid solution [25]. An increase above the cloud point may also cause polymer precipitation, which can result in an inactive KHI as the polymer becomes unavailable in the water phase to interact with the hydrate structure [26]. The lactam ring`s size impacts polymer performance; a larger ring increases hydrophobicity, decreasing the cloud point and enhancing the polymer performance [17].

Examples of poly(N-vinyl lactam) polymers (**Figure 1.5**) include five to eight-ring structures, whereas commercial polymers consist of five and six-ring structures. The five-ring structure is called polyvinylpyrrolidone (PVP). Increasing the ring size to six rings produces a polymer called polyvinylpiperidone (PVPip). A further increase in ring size to create seven and eight-ring structures results in the formation of two other lactam polymers: (poly(N-vinylcaprolactam)) (PVCap) and polyvinylazacyclooctanone (PVACO). Among these products, only PVCap and PVP are commercialized [24]. However, a problem with these commercial products is that they have a significantly low biodegradation rate (2% over 28 days), which sparks an interest in using environmentally friendly products such as polysaccharides and amino acids as alternative KHIs [27].

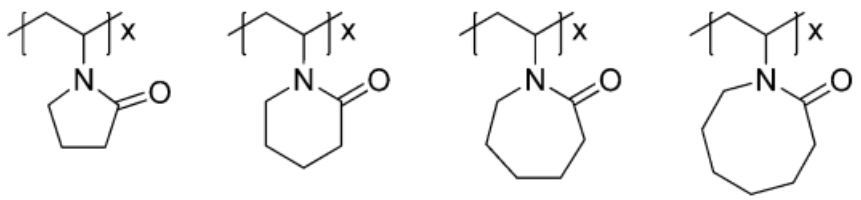

Figure 1.5 *Structural schematic of PVP (to the left), PVPip, PVCap, and PVACO [28].*

Besides increasing the lactam ring on these polymers to gain higher performance, one can also put alkyl groups on the lactam ring, as this causes a higher hydrophobicity [28].

PVP

PVP was discovered through anti-freeze protein studies on arctic fish species such as the winter flounder. The fish was able to survive in arctic areas below zero-degree temperatures as it had a special protein called Anti-Freeze Protein (AFP). The AFP has an affinity towards the nucleus on the ice surface and therefore prevents the fish from freezing to death [23]. Further studies on AFPs have shown that they are effective against sI and sII hydrates and can restrict the crystallization process inside the hydrate clathrate. They can also be classified as green hydrate inhibitors as they are non-toxic. An obvious problem with this biomolecule is its production and the need for large quantum. The AFP can be obtained from the organisms that produce them, by purification or be transferred as a DNA sequence into a host (e.g., bacteria, algae, plants, etc.) genome. None of these alternatives have been very successful [29] and the research is ongoing.

PVP is the first known kinetic hydrate inhibitor and is thought to be the industry standard when comparing the performance of nascent KHIs. The hydrate inhibition method of PVP is assumed to be surface adsorption by the pendant lactam groups on the hydrate surface [30]. The cloud point of PVP is above 100 ℃ which results in a reduced performance, compared to PVCap that have a cloud point of 31 ℃ [31] and thus provides a better performance.

PVCap

The Colorado School of Mines discovered PVCap in the early 1990s [23]. Due to its exceptional KHI performance, it is widely regarded as one of the industry standards for comparing newly synthesized KHIs in the laboratory [32]. The hydrate nucleation delay capacity of PVCap has been reported to be around 24 hours at a concentration of 5000 ppm and a subcooling of 8-9 ℃. Increasing the subcooling to 12 °C or higher renders the polymer ineffective [33]. The performance of PVCap is found to be concentration-dependent, where the optimum concentration is 5000 ppm. In an attempt to combine the excellent inhibitory effects of PVP and PVCap, copolymers known as vinyl pyrrolidone/vinyl caprolactam (VP/VCap) have been synthesized. The ratio of VP/VCap is important as a ratio of less than 25/75 results in comparable performance to PVCap when tested on its own [30]. The performance of PVCap can also be improved by adding synergists (typically nBGE) or by structure modification [33, 34].

PVACO

PVACO was first synthesized in 2012, and the performance was compared to PVP, PVPip, and PVCap in a five-cell rocking test. The results indicated that PVACO outperformed the other tested polymers and that the KHI performance increased as the size of the lactam ring increased [35]. A more recent study utilizing molecular simulations and calculations reached the same conclusion, finding that PVACO exhibited the highest performance. A general KHI adsorption theory was proposed; hydrate growth was delayed due to the adsorption of the lactam ring onto the hydrate cage as the lactam ring fitted well onto the cage, and the presence of carbonyl groups on the lactam rings resulted in hydrogen bonding with water molecules on the hydrate cage. It was also suggested that PVACO and PVCap outperformed PVP and PVPip due to the carbonyl oxygen atom on the lactam ring. A larger lactam ring resulted in the formation of two hydrogen bonds from the oxygen carbonyl group, one with the solution itself and one with the hydrate cage. Meanwhile, PVP and PVPip only formed one hydrogen bond with the water molecules on the hydrate cage [36].

1.6.1.2 Hyperbranched Polyesteramides

Hyperbranched polyesteramides (**Figure 1.6**) belong to another class of commercial KHIs. They can obtain a subcooling of around 10 ℃, which is similar to VCap polymers [17]. The synthesis of hyperbranched polyesteramides results in a polymer that has hydroxyl groups at the endpoints. The endpoints of the polymer can be tailor-made to become more hydrophobic or hydrophilic by adding, e.g., a secondary amine to the reaction mixture. Similar to the poly(N-vinyl lactam) polymers, the hyperbranched polyesteramides also have an amide group with a hydrophobic group attached. The hydrophobic group interacts with the hydrate surface through Van der Waals forces, and the amide groups help to attach to water molecules on the hydrate surface via hydrogen bonding. Hyperbranched polyesteramides are different from the previously mentioned classes as they exhibit a hyper-branching ability, which allows them to bind in several places on the hydrate surface compared to the other classes that will bind to a single place on the hydrate surface [23]. The hydrophilicity of the molecule is owed to the hydrophobic cyclohexyl rings and the hydrophilic amide groups [17].

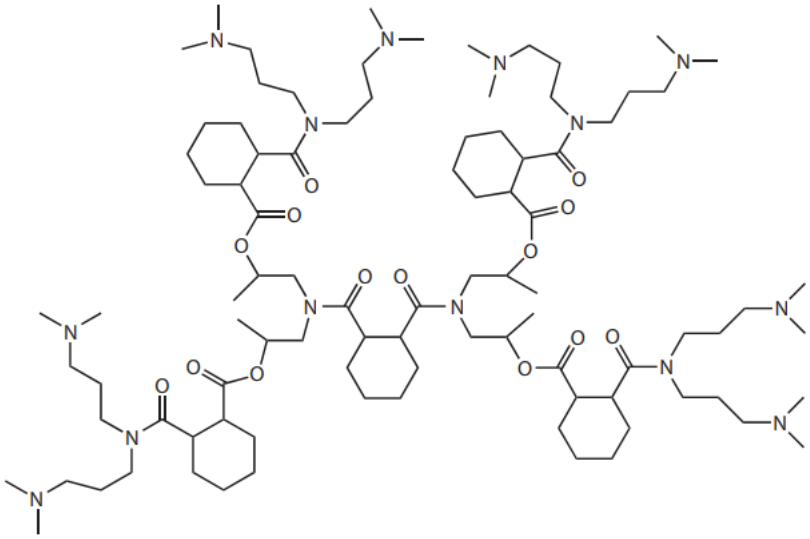

Figure 1.6 *Structural schematic of a hyperbranched polyesteramide [17].*

1.6.1.3 Isopropylmethacrylamide Polymers

This class of polymers is based on acrylamide polymers. A way to characterize polyvinyl-based polymers is by using their tacticity. Tacticity can be defined as the relative stereochemistry of adjacent monomer units. There are three different types of tacticities: Isotactic, syndiotactic, or atactic. The isotactic type is characterized by the pendant groups being placed on the same side of the polymer chain. Meanwhile, the syndiotactic pendant groups are placed in an alternating pattern on the polymer chain. For the atactic type, the pendant groups are placed in a randomized order. A study with poly N, and N-dialkyl acrylamides showed that the syndiotactic polymers gave a better KHI performance compared to the other tacticities [37]. Poly(N-isopropyl acrylamide)s (PNIPAM)s (**Figure 1.7**) have been investigated as a potential KHI, and the reported results were that tacticity plays a role in KHI performance as the PNIPAM with a higher syndiotactic percentage performed better than the PNIPAM with a lower percentage [38].

PNIPMAm

An example of a commercially available KHI within the isopropylmethacrylamides is the poly(N-isopropyl methacrylamide) (PNIPMAm) (**Figure 1.8**). Its performance varies depending on the polymer molecular weight, synthesis method, and the presence of synergists [39].

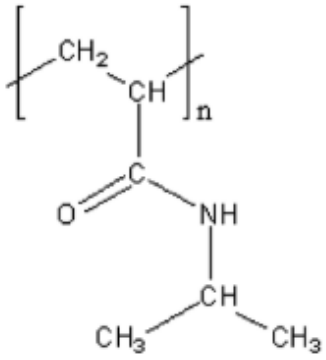

Figure 1.7 *Structural schematic PNIPAM [38].*

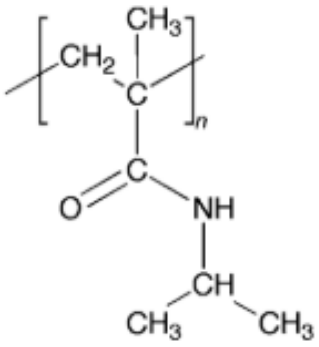

Figure 1.8 *Structural schematic of PNIPMAm [37].*

The presence of the methyl groups on the polyvinyl backbone contributes to the KHI performance. By unfolding the polymer structure, the methyl groups increase the ratio of surface area to volume, making a larger portion of the polymer structure available for interaction with the bulk water [40].

1.6.1.4 Amine Oxides

As previously mentioned, the main ingredients in a commercial KHI are a water-soluble polymer and the presence of amphiphilic groups. The amphiphilic groups usually consist of an amide and a hydrophobic group that is conventionally bonded directly to the amide group [41]. Examples of these components are shown in **Figure 1.5**.

Amine oxides have a structural similarity to amides and quaternary ammonium salts (**Figure 1.9**), as the nitrogen atom in the structure can attract four different groups [41]. An amine oxide can be synthesized by reacting hydrogen peroxide with tertiary amines. This KHI group is versatile as it has a wide range of uses. It can be used as surfactants in cleaning products, foam stabilizers, anti-static agents in the textile industry, and even in deodorant bars as an anti-bacterial agent. The amine oxides are also quite environmentally friendly as the bioaccumulation potential is low in aquatic organisms [42]. Studies have also shown that they are easily biodegradable under anaerobic and aerobic conditions [43].

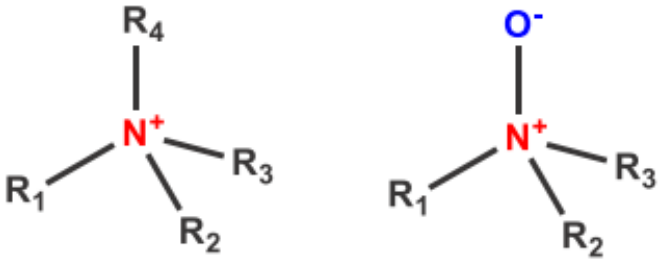

Figure 1.9 *General structural schematic of quaternary ammonium salt (to the left) and amine oxide (to the right) [41].*

According to molecular studies, butyl and pentyl groups work best as hydrate inhibitors compared to the other n-alkyl groups, as these groups can penetrate the cavity on the surface of the $5^{12}6^4$ sII hydrate. This is also confirmed in a study performed on tetrahydrofuran (THF) hydrate, with tri-n-butyl amine oxide (TBAO), tri-iso-pentyl amine oxide (TiPAO), and tri-n-pentyl amine oxide (TPAO). THF hydrate is comparable to sII hydrates. The results showed that the butylated alternative performed best as the nitrogen atom in the amine oxide was closer to the $5^{12}6^4$ sII cage which resulted in stronger van der Waals interactions between the amine oxide and the hydrate cavity [44].

Previous studies have indicated that dibutyl amine oxide serves as an internal synergist, enhancing the performance of other polymeric categories [45]. Furthermore, the chemical structure of the amine oxide also plays a role in the KHI performance. The negatively charged oxygen atom in the amine oxide structure is believed to provide increased hydrogen bonding abilities, through interaction with the hydrate surface or the bulk water [41]. A study with THF-hydrate crystal growth showed that the linear amine oxides exhibited a better KHI performance than the branched versions in regards to slowing down crystal growth. The suggested mechanism was that the branched polymers may contribute to steric hindrance where the interaction between the hydrate surface and the polymer is not as good [46].

Polyamine oxides

KHI performance testing on non-polymeric amine oxides (**Figure 1.10**) has been reported to result in poor performance [44]. However, if the amine oxide is modified through polymerization, the performance is enhanced, especially when butyl groups are attached. The increased performance due to polymerization is proposed to correspond to the presence of additional oxygen atoms. A larger number of oxygen atoms results in a stronger hydrogen-bonding ability which leads to a larger perturbation of the bulk water [47]. Previous work by

Zhang et al. concluded that their performance can be comparable to PVCap at a 2500 ppm concentration [48].

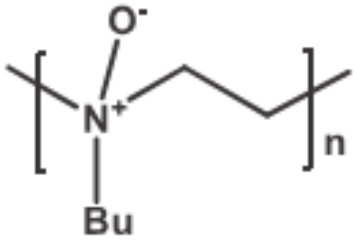

Figure 1.10 *Structural schematic of a polyamine oxide [41].*

One of the main topics of this thesis is to investigate the KHI performance of a brand new class of polymers called polyvinyl amine oxides (**Figure 1.11**). This class has never previously been synthesized or tested for its KHI performance.

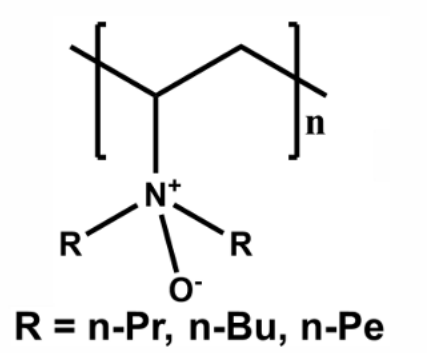

Figure 1.11 *Structural schematic of a general polyvinyl amine oxide. The side group, R, can be varied by the addition of propyl, butyl, or pentyl groups. The structure was drawn using the ChemDraw Professional software.*

1.6.1.5 Poly(2-dialkylamino-2-oxazoline)s

In the mid-1960s, a new class of polymers called poly(2-alkyl/aryl-2-oxazoline) (PAOx) was discovered. This polymer class was found to possess unique properties such as a versatile structure, good biocompatibility, and adjustable crystalline and thermal behaviors. In addition, the properties could also be customizable. The structure of the 2-oxazoline (**Figure 1.12**) consists of a five-membered heterocyclic imino ether. Modification of the substituent at the 2-position allows for the change of mechanical, thermal, and solution properties [49]. Furthermore, poly(2-alkyl-2-oxazoline)s are a subclass of polyamides, where the structure is based on tertiary amides. Previous testing of the poly(2-alkyl-oxazoline) class indicated that a copolymer consisting of 2-methyl-2-oxazoline and 2-iso-butyl-2-oxazoline had a performance

similar to the copolymer N-vinylpyrrolidone-N-vinyl caprolactam (VP/VCap). The drawback of the poly(2-alkyl-2-oxazoline)s is their poor biodegradability [50].

Figure 1.12 *Structural schematic of poly(2-alkyl-2-oxazoline)s [51].*

However, a new subclass of the poly(2-oxazoline)s called poly(2-dialkylamino-2-oxazoline)s (PAmOx) (**Figure 1.13**) has been recently discovered in collaboration with the Hoogenboom group in Belgium. PAmOx is structurally related to the 2-dialkyl-2-oxazolines, as the synthesis is based on the polymerization of monomer units of this compound. In a recent study, the performance of the poly(2-dialkylamino-2-oxazolines) was examined with the slow constant cooling test method (explained in a later subchapter). The study's findings indicated that polymers containing ring structures, such as pyrrolidine and piperidine, demonstrated the highest level of effectiveness. The study also suggested that the presence of pendant alkyl groups influenced the performance of the KHIs and it was further suggested that these groups should be in close proximity to other groups capable of forming strong hydrogen bonds. Furthermore, altering the size and shape of the alkyl groups could potentially lead to improved performance. Additionally, some of the polymers showed performance similar to PVCap [51]. The poly(2-dialkylamino-2-oxazoline)s are one of the main topics in this thesis and will be discussed later in more detail.

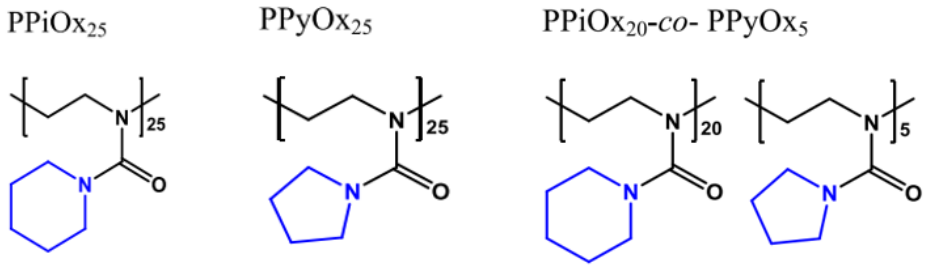

Figure 1.13 *Structural schematic of different polymer structures of poly(2-dialkylamino-2-oxazoline)s [51].*

1.6.2 KHI Mechanisms

A specific mechanism of how KHIs work to inhibit hydrate formation is yet to be defined, and the existing theories can be viewed as hypotheses. The four existing hypotheses are adsorption inhibition, perturbation inhibition, crystal growth inhibition, and interference with the hydrate nucleation site. The following subchapters will be dedicated to all four hypotheses [24].

1.6.2.1 Adsorption Inhibition

The mechanism of adsorption inhibition suggests that the KHI molecules adhere to the surface of the crystal aggregate through adsorption (**Figure 1.4**), thereby interrupting the process of hydrate nucleation. This theory is supported by many experimental studies [24]. Yagasaki et al. conducted a study on the growth of the ethylene oxide hydrate (which is comparable to sI hydrate) in combination with the KHIs, PVCap, and AFP. The research group discovered that the AFP preferred a specific plane of ice to adsorb to. In addition, it was proposed that PVCap irreversibly adsorbed on the hydrate surface only when two lactam rings were confined in the open hydrate cages [52]. The proposed general adsorption mechanism is also supported by Zhang et al. where the authors claim that PVP and PVCap adsorb onto cyclopentane hydrates by forming hydrogen bonds with pendant hydrogen atoms at the hydrate surface and the oxygen atom that resides on the cyclic amide group of the inhibitor molecule [53].

1.6.2.2 Perturbation Inhibition

The perturbation inhibition method (**Figure 1.4**) suggests that the KHIs molecules are able to perturb the water phase, resulting in incomplete cages of host water molecules [24]. A molecular dynamics study by Li et al. provides valuable insight into this theory as the introduction of a KHI (PVP-A, PVP-E, and PVP) resulted in the formation of strong inter-molecular hydrogen bonds between the double bond oxygen atoms on the KHI and the hydrogen atoms of the surrounding water molecules [54]. This means that the KHI mimics the host water lattice's structure, attracting even more water molecules with hydrogen bonds and disturbing the hydrate particle's continuous growth.

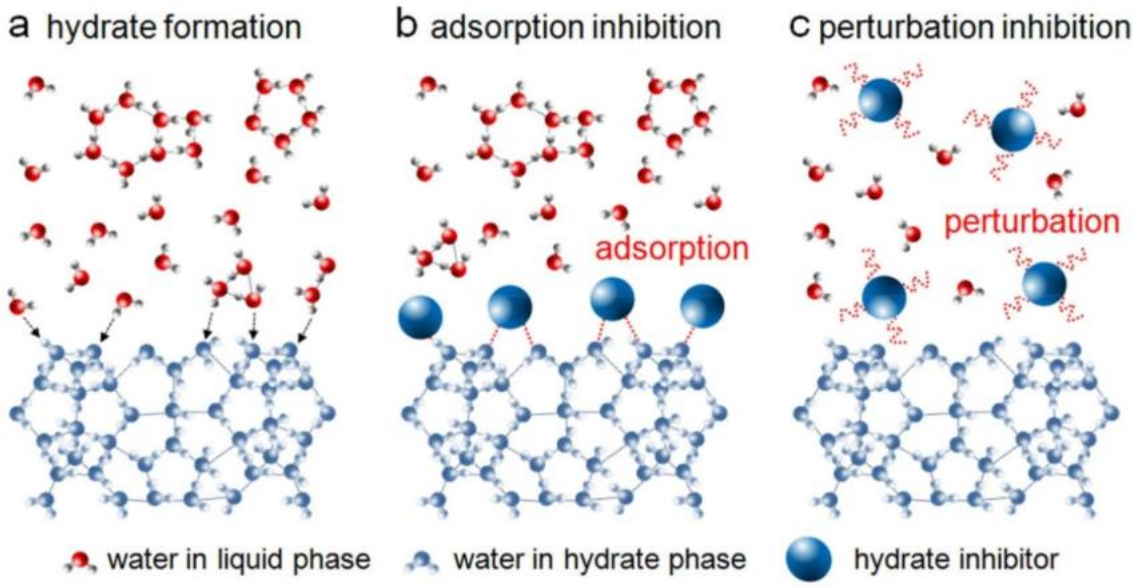

Figure 1.14 *Schematic molecular overview on hydrate formation and inhibition by adsorption and perturbation mechanisms [19].*

1.6.2.3 Crystal Growth Inhibition

Induction time studies have been developed as the main method for testing and developing KHIs as they represent the timeframe between when the hydrate stability zone has been achieved and the subsequent formation and growth of the hydrate. The basis for this theory assumes that the KHI adsorbs to the hydrate nuclei and thus hinders further growth. However, such studies have been reported to be stochastic as the nucleation mechanism of hydrate formation is regarded as a sensitive parameter. Therefore, a new method called the Crystal Growth Inhibition (CGI) method was developed to try to overcome this. The first step in the CGI method is to cool the system to temperatures at which hydrate formation can occur. The next step is then to heat up the system in order to dissociate the hydrate crystals formed in the first step. The last step involves cooling down the system to a hydrate-forming temperature again, but this time, a small sample of the hydrate formed in the first step is kept inside the system. Keeping a small amount of hydrate "seed" in the system eliminates the uncertainties and stochasticity associated with primary nucleation, as the KHI polymer interacts only with pre-existing hydrate particles that are thermodynamically stable and not recently formed ones [14, 55].

1.6.2.4 Interference with Hydrate Nucleation Site

Perhaps a less widely recognized inhibition mechanism is that the KHI polymer chains either interfere with or cover nucleation sites, which, according to Ke et al., has been supported by two studies [24]. A study performed with AFPs as a KHI on THF hydrates suggested that the AFPs adsorb to the surface of nucleating impurities of the hydrate-forming solution and, thus, preventing heterogeneous nucleation from occurring [56].

1.6.3 Effect of Synergists

A common problem with injecting a KHI alone into a pipeline is that the hydrate delaying performance declines under high subcooling conditions. This is because the driving force for hydrate formation is greater, leading to a higher likelihood of hydrate formation. An alternative solution to circumvent this problem is to add a synergist to improve the KHI performance [57, 58]. The synergist is added with one or more solvents to liquefy the KHI formulation, making it easier to pump through the pipeline [59]. A synergistic effect occurs when two or more substances interact to produce a greater combined effect than when separated [60]. The main goal of the synergist addition is to delay the onset temperature at which hydrates form [61]. However, the mechanism(s) of how the synergists work is not yet fully understood where some theories state that the synergist and KHI polymer present a co-adsorption effect on the hydrate surface along with the water perturbation theory or that there exists a cooperative mechanism between the KHI itself and the synergist where the water molecules are subjected to perturbation [62].

Glycol ether compounds, polyethylene oxide, and quarternary ammonium salts are the most widely studied synergists [61].

1.6.3.1 Mono-n-butyl glycol ether

Mono-*n*-butyl glycol ether (nBGE) (**Figure 1.15**) is a widely known synergist for PVCap and other types of KHIs [62] . Despite its widespread use, the exact mechanism of how the nBGE interacts with the KHI polymer is still unknown. One proposed mechanism is that the nBGE acts as a stabilizing agent for the KHI polymer at the interface between water and hydrate, and some claim that it can enhance the adsorption effect of the KHI [39].

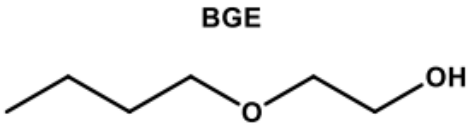

Figure 1.15 Structural schematic of nBGE [62].

1.6.3.2 Isobutyl glycol ether

The addition of isobutyl glycol ether (iBGE) (**Figure 1.16**) has previously demonstrated good synergy when combined with PVCap or PNIPMAm. It is suggested that a tail-branched alkyl group functions more effectively than a straight chain [59]. Similar to nBGE, there is no defined mechanism of how this glycol ether works either. It has been suggested that the branching of the glycol ether increases its adhering capacity to the hydrate surface and that the branching also disrupts the adjacent water molecules [63].

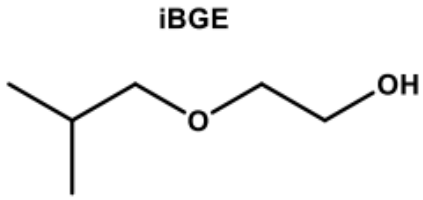

Figure 1.16 *Structural schematic of iBGE [62].*

1.6.3.3 Dipropylene glycol butyl ether

Another solvent synergist from the glycol ether category is dipropylene glycol butyl ether (DPBGE). The mechanism of DPBGE (**Figure 1.17**) is not yet fully understood (as for the other glycol ether compounds). The hypotheses range from synergist adsorption on the hydrate surface, to perturbation of the water molecules, to a decrease in the interfacial tension between liquid and gas [34]. The addition of DPBGE with PVCap has shown outstanding results. A possible explanation for why it works so well is because it is a mixed compound, which means that it can interact with the water and hydrate surface in multiple ways. The compound is also less water soluble due to the hydrophobic methyl side groups and butyl group, which may have an impact on the cloud point as polymers with low cloud points display better performance, according to previous studies [62].

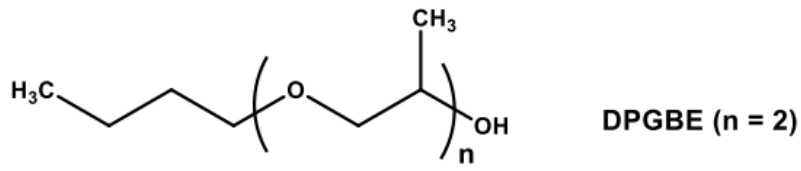

Figure 1.17 *Structural schematic of DPBGE [62].*

1.6.3.4 Tri-iso-pentyl amine oxide

The synergist tri-iso-pentyl amine oxide (TiPeAO) (**Figure 1.18**) is a member of the trialkyl amine oxides, which have been demonstrated to have good synergistic abilities in combination with KHIs [64]. The inhibition mechanisms for amine oxides are assumed to be the formation of hydrogen bonds between the clathrate and the amine oxide group combined with alkyl groups that penetrate the exterior of the hydrate [60]. A recent study with a mixture of PNIPMAm and TiPeAO showed that the blend was effective at various concentrations, but overdosing the blend (e.g., 5000 ppm of each chemical) resulted in worse results. A possible explanation for the poor results at higher concentrations is aggregation between the amine oxide and the polymer [64].

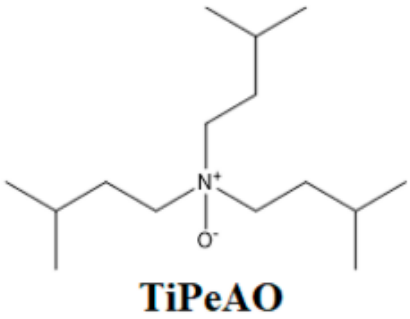

Figure 1.18 *Structural schematic of TiPeAO [64].*

1.6.4 KHI Performance Test Methods in the Laboratory

1.6.4.1 Slow Constant Cooling Test

The slow constant cooling (SCC) test is a test method used for performance screening of the KHIs [65]. The test involves inserting the KHI solution into a 40 mL high-pressure steel rocking cell with a steel ball contained inside the cell. Prior to initializing the test, each cell is pressurized with approximately 76 bar of synthetic natural gas (SNG). The start temperature

of the test is 20.5 °C, as this represents the hydrate equilibrium temperature at 76 bar of pressure. After the test is initiated, the temperature and pressure start to decrease at a constant rate (1 °C per hour) over approximately 18.5 hours, with the minimum temperature set to 2 °C. The pressure and temperature data for each cell is logged on a computer as a pressure/temperature versus time graph. The first sign of a deviation in the pressure curve due to a drop in temperature marks the onset temperature T_o, which can be regarded as the temperature where the first hydrates start to form. As time goes on, the pressure curve starts to deviate even further, and the steepest deviation on the pressure curve can be interpreted as the T_a, which is the temperature where rapid hydrate formation occurs. The T_o value can then be subtracted from the T_a value to find the anti-hydrate formation ability of the tested KHI [35, 66]. The SCC test can also be performed with methane gas, but then at a 110 bar pressure [64].

The test simulates the pipeline conditions as the steel ball causes strong turbulence and shear forces thereby mixing the aqueous volume and the test gas as it moves across the length of the cell [67].

1.6.4.2 Crystal Growth Inhibition Method

The Crystal Growth Inhibition Method (CGI) was originally made to bypass the stochastic nature of hydrate nucleation and shift the focus to the inhibition properties of the KHIs that could easily be quantifiable. The test induction starts with supplying gas (North Sea natural gas) to high-pressure autoclave cells at a temperature outside the hydrate-forming region and is followed by a rapid cool-down of the system to ensure that rapid hydrate formation occurs in the system. The system is then warmed up in a stepwise process to ensure the dissociation of nearly all hydrate particles. Furthermore, the temperature in the cell is cooled down at a constant rate of 1.0 °C per hour to assess how changes in the hydrate growth rate correlate to the subcooling. The heating and cooling cycles are then repeated multiple times to assess the reproducibility [68]. Following the final heat cycle, the cell is cooled down in steps while retaining a small fraction of hydrate inside the cell. The main objective of the method is to identify regions with slow growth and complete inhibition of the hydrate particle. The final step is an analysis of the pressure and temperature data obtained from these cooling/heat cycles to depict where the crystal growth inhibition regions are [14].

1.6.4.3 Isothermal Method

The isothermal method (**Figure 1.19**) has a similar setup to the SCC test, where the testing equipment is a five-cell high-pressure rocker rig. Unlike the SCC test, the agitation of the cells and the subsequent initiation of the test do not occur before the cells are cooled to a pre-defined temperature (e.g. 7 °C) and the test pressure is at approximately 68 bars. The system is then held at this temperature until hydrate formation occurs. The induction time, t_o, represents the time it takes (in minutes) from rocking is initiated to the point where the first significant pressure drop occurs and the initial hydrate particles start to form. The t_a is defined as the fastest time for hydrate growth, e.g., the point of the steepest decline of the pressure curve [69, 70].

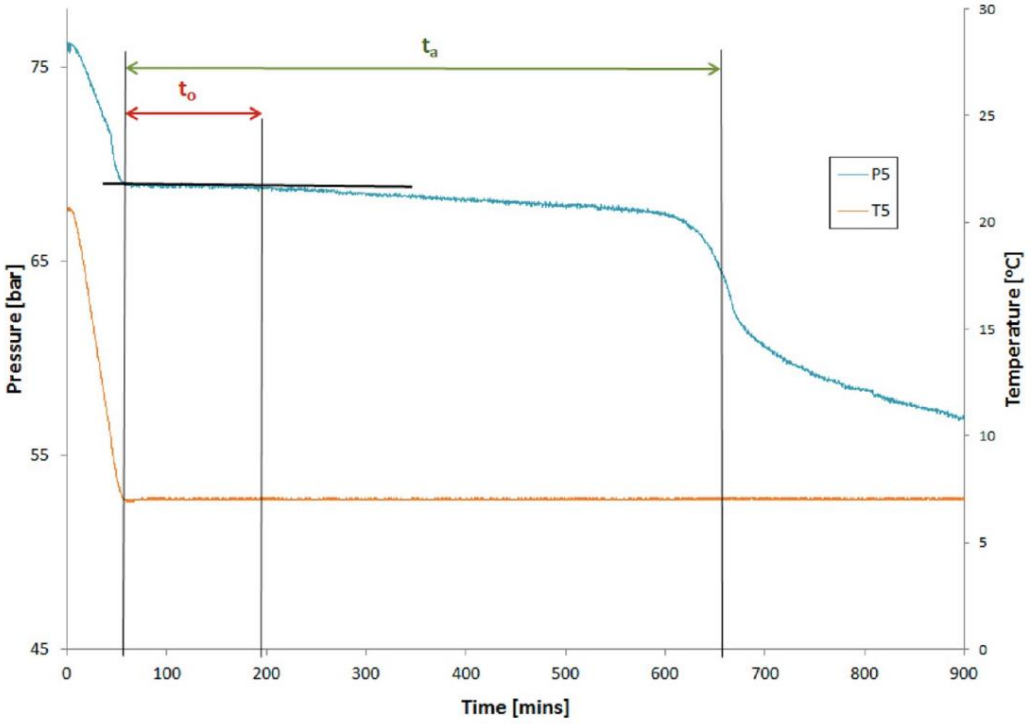

Figure 1.19 *Visual representation of the pressure (P5) and temperature (T5) graphs obtained with the isothermal method and how to graphically derive the t_o and t_a values [69].*

1.6.4.4 Ramping Method

The ramping method (**Figure 1.20**) involves introducing the cells to a stepwise cooling regime. At first, the cells are cooled down to a specific subcooling with agitation. Then, the subcooling temperature is held for some time (a few hours) before the system is cooled even further down to a higher subcooling with a hold time. The temperature ramping continues until the formation of hydrates occurs [70]. A more detailed explanation of the ramping method is provided by Villano et. al [50].

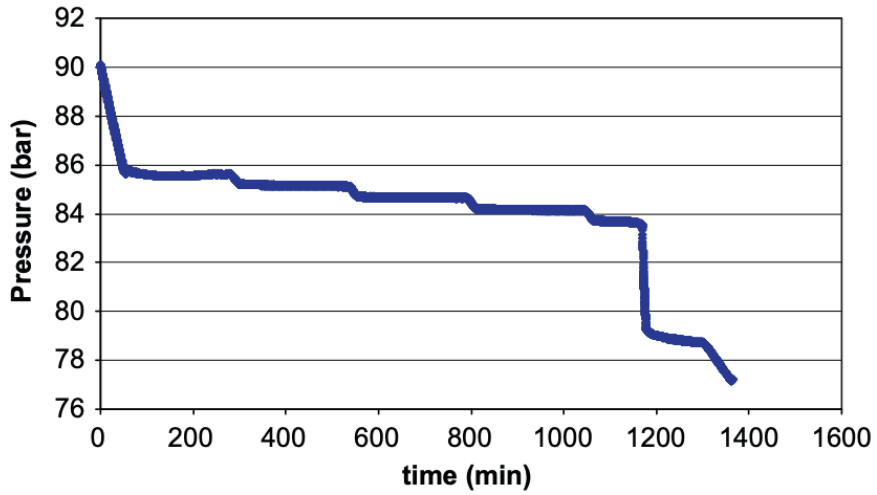

Figure 1.20 *Schematic representation of the ramping method [70].*

1.7 Main Objectives of Thesis

The main objectives of this thesis were to design and test the performance of two types of kinetic hydrate inhibitors. This thesis consists of two main projects: polyvinyl amine oxides and poly(2-dialkylamino-2-oxazoline)s. The focus on developing a new class of amine oxides was to try and meet the need in the LDHI industry for commercially available alkylated amine oxides (with good KHI performance) that can be synthesized in large quantities [41].

The reason for also having a focus on the poly(2-dialkylamino-2-oxazoline)s was to explore this new and promising KHI class even further, with the addition of synergists, and also to test its performance in methane gas [51].

2 Experimental Methods

This chapter contains the synthesis of the polyvinyl amine oxides, sample preparation for the performance testing, a detailed explanation of how the performance testing was conducted with the constant cooling method and the isothermal method, and the strategy for interpreting the test results from the graphs obtained by these methods. The last section describes how the polymer characterization was conducted.

2.1 Synthesis of Polyvinyl Amine Oxides

Various versions of polyvinyl amine oxides have been synthesized. The alkyl group has also been varied. Most of the syntheses have been based on the solvent isobutyronitrile (iPRCN), but attempts have also been made using acetonitrile as a substitute. Proton (^{1}H) NMR was conducted on several products to confirm their chemical structure (see appendices A and B for NMR graphs). The solvent for the NMR samples was either dimethyl sulfoxide (DMSO) or chloroform-D ($CDCl_3$).

2.1.1 Synthesis of Polyvinyl Dibutyl Amine Oxide: A Low M_w Example

Materials:

The polyvinyl amine was supplied by BASF SE under the trivial name Lupamin 1595 (M_w= 10 000 g/mol, pH= 7.5) in a 10-weight percent aqueous solution and came in the form of a hydrochloride salt [66]. The solvents 1-bromobutane (BuBr), isobutyronitrile, and sodium hydroxide (NaOH) (in the form of pellets for analysis EMSURE®) were all supplied by Merck Life Sciences AS. No further modifications of the solvents were made. Isopropanol (iPrOH) was supplied by KiiltoClean, and the hydrogen peroxide (H_2O_2) was supplied by VWR. Both solvents were used as received from the suppliers. Anhydrous sodium sulfate was added as a dehydrator and used as received from the supplier (Merck Life Science AS).

Methods:

Step I: Converting the polymer to a polyvinyl dibutyl amine

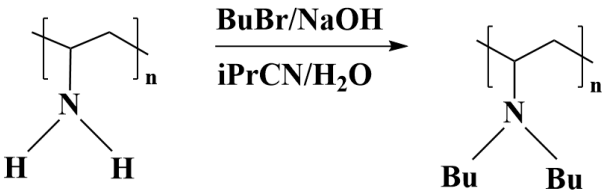

Figure 2.1 *The first step of polyvinyl dibutyl amine oxide synthesis. Protons are substituted with butyl groups. The structures were drawn with the ChemDraw Professional software.*

The first step of the reaction (**Figure 2.1**) involved adding five grams of polymer (Lupamin 1595, 10 wt.%) to a round bottleneck flask, following a 10-gram addition of deionized water. Subsequently, 1.304 grams of sodium hydroxide was added to the solution, and a heat gun (Cocraft) was used to dissolve the sodium hydroxide pellets. Furthermore, approximately 10 mL of iPrCN and 3.346 grams of bromobutane were added to the flask. A layer separation occurred where two layers were visible: a light orange-brown color in the top layer and a darker orange-brown color in the bottom layer. A magnet was then put in the flask, and the mixture was then subjected to overnight reflux in an oil bath of 71°C with stirring.

Step II: Converting the polyvinyl dibutyl amine to a polyvinyl dibutyl amine oxide

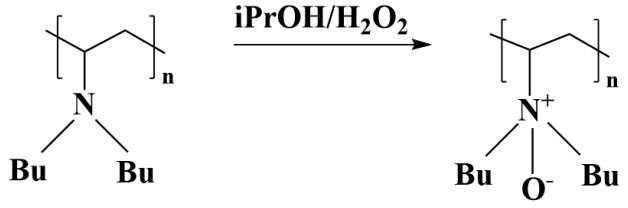

Figure 2.2 *The second step of the polyvinyl dibutyl amine oxide synthesis. The oxidation led to the incorporation of the amine oxide group (N^+-O^-). The structures were drawn with the ChemDraw Professional software.*

The second step involved oxidizing the polyvinyl dibutyl amine (**Figure 2.2**). Following the overnight reflux, the magnet was removed, and the solution was added to a separating funnel. Two layers emerged due to gravity separation: a top layer (product phase) and a bottom layer (water phase). The water phase was carefully separated into a beaker and set aside. Subsequently, the remaining layer (product phase) was extracted in a separate beaker. Following this, the water phase was put back into the separating funnel and subjected to a 10-15 mL addition of iPrCN in order to increase the product yield. Finally, the water and product phases were transferred back into their respective beakers.

Moreover, a small amount of sodium sulfate was added to the product to remove solids and water. A florentine was taken out, and the weight was noted down before the product was decanted into the florentine. The product was then subjected to rotation and evaporation on a rotavap (BÜCHI Rotavapor R-200) with an adjoining heating bath (BÜCHI Heating Bath B-490) at 70 °C. The rotary evaporation was performed multiple times until a constant product weight of approximately 0.5 grams was obtained.

Following the rotary evaporation, a small amount of isopropanol (3-4 mL) was then added to the product, and the mixture was heated with a heat gun. Lastly, hydrogen peroxide was

added in a 30-weight percent concentration along with a magnet. The florentine was then capped and put on a stirrer overnight. The weight percentage of the $PVAmBu_2O$ was calculated the next day, and the solution was bottled up in a small glass container and labeled before it was tested on either of the rocker rigs.

2.1.2 Synthesis of Various Versions of Polyvinyl Amine Oxides

Versions of medium and high molecular weight polyvinyl dibutyl amine oxides were also synthesized. The polyvinyl amines of medium and high molecular weight were supplied by BASF and had an aqueous weight percent of 11. The high molecular weight polyvinyl amine went under the tradename Lupamin 9095 (M_w = 340 000 g/mol, pH= 7.5), while the medium molecular weight polyvinyl amine was named Lupamin 5095 (M_w = 45 000 g/mol, pH= 7.5).

A propyl version of the polyvinyl amine oxide was also synthesized with 1-PropylBr (VWR) as a solvent. A pentyl version was also attempted with 1-bromopentane (TCI) as a solvent. Both were synthesized with the low molecular weight Lupamin 1595.

Versions of $PVAmBu_2O$ with $NaHCO_3$ (VWR) and Na_2CO_3 (VWR) were also attempted. Other modifications were made to the synthesis of polyvinyl butyl amine oxide, including altering the butyl group to be monobutylated or tributylated. There were also attempts to substitute the solvent iPRCN with acetonitrile (Carl Roth®). A N-isopropyl-3-isopropyl amino-propanamide synthesis was also explored. The $PVAmBu_2O$ synthesis was also varied with different mol fractions of NaOH and BuBr.

2.2 Polymer Characterization

^{1}H NMR (see **Appendix A** and **Appendix B**) was performed on several of the synthesized products (prior to reacting with hydrogen peroxide) in order to examine the purity and molecular structure of the polyvinyl amine samples. The NMR samples were prepared by extracting a small sample of the product (~10 mg) (after rotary evaporation) and dissolving it in 0.5 mL solvent (DMSO or $CDCl_3$, depending on the sample). Both solvents were supplied by VWR. The sample was then transferred into an NMR tube using a glass pipette (VWR). Subsequently, it was placed in the sampler unit (Bruker SampleXpress) and run on the NMR instrument (Bruker Ascend^{TM} 400) (**Figure 2.3**) connected to the sampling unit. After completing the analysis, the software (Bruker TopSpin 3.5) generated the NMR graph for the specified sample.

Figure 2.3 *NMR instrument and sampler unit.*

2.3 Performance Testing in the Laboratory

2.3.1 Slow Constant Cooling Test

SNG and methane tests were performed on two identical rocker rigs, RC5-1 (SNG) and RC5-2 (Methane). The KHIs tested were polyvinyl amine oxides and poly(2-dialkylamino-2-oxazoline)s.

2.3.1.1 SNG as Test Gas

The performance testing of the different KHIs was conducted using the high-pressure rocking cell RC5 equipment (PSL Systemtechnik, Germany) (**Figure 2.4**), which contains five parallel rocking cells (Swagelok, Norway) and an adhering temperature-controlled water bath (Huber). The content of the water bath was a mixture of ¼ of MEG (VWR) and ¾ of deionized water. The SNG (**Table 2.1**) was supplied by Nippon Gases. The hydrate equilibrium temperature was previously determined by Calsep`s PVTSim software to be 20.5 °C when the hydrate is a structure II hydrate with an SNG pressure of 76 bar [51]. The software connected to the rocker rig was programmed to rock the cells at a rate of five rocks per minute with an angle of 40 °C.

The slow constant cooling method on the RC5-1 was programmed to perform a step-wise cooling and heating cycle where the start temperature of the test was 20.5 °C. At the test initiation, the temperature decreased from 20.5 °C to 2.0 °C over a period of 18.5 hours. Subsequently, the temperature was maintained at 2.0 °C for one hour, before being raised to 25.0 °C over the course of an hour. Following this, the temperature was decreased from 25.0 °C to 20.5 °C over a period of 20 minutes. Finally, the temperature was held at the hydrate equilibrium temperature of 20.5 °C for several hours. The rate of cooling was 1°C per hour. One test (e.g., one five-parallel run) took around 23 hours to complete.

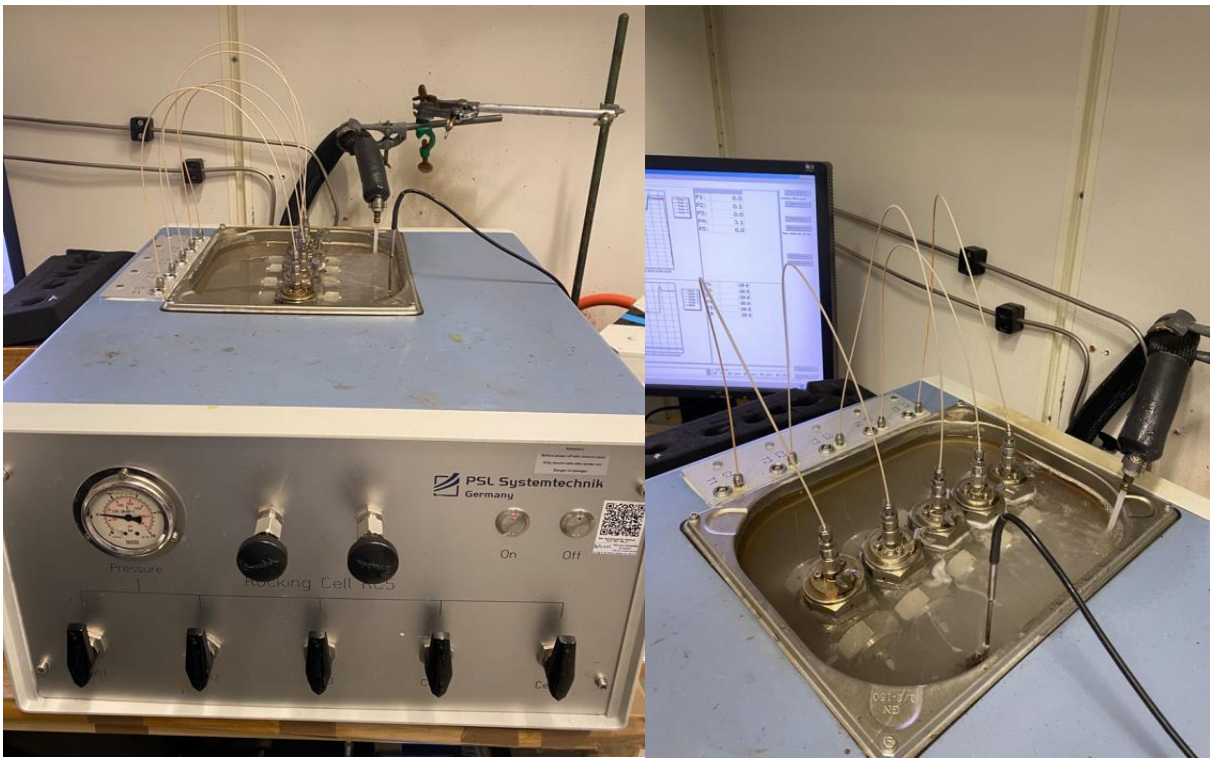

Figure 2.4 *RC5 five-cell high-pressure rocking test equipment.*

Table 2.1 *Composition of SNG mixture used in the rocking cells [43].*

Gas component	**Mol percentage**
Methane	80.4
Ethane	10.3
Carbon dioxide	1.82
Propane	5.00
Isobutane	1.65
n-Butane	0.72
Nitrogen	0.11

Sample preparation:

The polyvinyl amine oxide sample preparation involved preparing a polymer solution consisting of 105 mL of deionized water and the desired polymer solution weight to obtain the right test concentration. A magnet was added, the test beaker was wrapped with parafilm, and the mixture was magnetically stirred for a few hours or overnight depending on how soluble the sample was. The test volume per cell was 20 mL.

The poly(2-dialkylamino-2-oxazoline)s were received in a powdered form from the Hoogenboom group in Belgium. The samples were prepared by weighing the desired amount of polymer in a beaker and adding 55 mL of deionized H_2O to it. A magnet was then added to the beaker, and the solution was magnetically stirred over a few hours with parafilm wrapped over the beaker until the polymer was completely dissolved in the water. The test volume per cell was 10 mL.

The synergist additions of nBGE (ALDRICH®), iBGE (TCI), and DPBGE (Avantor/VWR) were added to the samples either by directly pipetting the synergist volume into the cell or by mixing it with the polymer test volume before transferring the sample into the cell with a graduated measuring cylinder (VWR).

The 3 wt.% sodium chloride solution was prepared by mixing 6 grams of NaCl (VWR) with 150 mL of deionized water. The mixture was stirred until the NaCl dissolved, and then additional deionized water was added to bring the total solution weight to 300 grams. In the sample preparation, the deionized water was substituted by the 3 wt.% NaCl solution.

The PVCap used in this thesis was supplied from BASF with the name of Luvicap EG HM with a molecular weight of 10 000 g/mol. The monoethylene glycol solvent was removed by repeated precipitation from a dilute aqueous solution at approximately 50 °C, resulting in a dry powder of pure PVCap polymer [63, 71].

General slow constant cooling test procedure with SNG:

1. A volume of 20 mL or 10 mL (depending on the test) of the prepared sample was carefully measured in a graduated measuring cylinder and placed into each cell containing a steel ball.

2. The cells were placed into their fixed position on the rocker rig, and the pressure/temperature sensor clip was locked onto each cell.

3. All cells were then subjected to a vacuum using a vacuum pump for 3 minutes to eliminate any gas from the system.

4. Following vacuuming, the outlet valve on the rocker rig was closed, and a small amount of SNG (10-20 bars) was applied to the cells by opening the valve on the SNG bottle.

5. The valve on the compressor unit (AEROTEC) was then turned on to supply an outlet pressure of 120. Then, the RC Control panel valve was opened prior to opening the valve marked “gas out.” (**Figure 2.5**).

6. The inlet valve on the RC5-1 unit was opened to allow the SNG to enter the cells.

7. After adding 10-15 bars of SNG, the inlet valve was closed, and the rocking motor was started on the computer software. The meaning behind this step was to disperse the gas inside the liquid cell volume.

8. After 3-5 minutes of rocking, the motor was stopped by clicking “stop” on the computer screen, and the gas was depressurized to zero bar pressure (by turning on the outlet valve) for all cells.

9. Following the depressurization, another round of vacuum was applied to all cells for 3-5 minutes.

10. The cells were then re-pressurized to 80 bars with SNG over several stepwise procedures (described in steps 4, 5, and 6), and the rig`s rocking motor was started using computer software. The rocking proceeded for 2 minutes.

11. The final step involved turning on the outlet valve to reduce the gas pressure from 80 to 76 bar.

12. After the obtainment of 76 bar pressure, the valve on each cell was closed, and the target and set temperature of the new test were manually set to 2.0 °C and 20.5 °C on the WinRC computer software.

13. The final step involved clicking the "start autorun" button on the computer software, which caused the cells to begin rocking. The computer recorded pressure and temperature data for each cell.

14. After the test was completed, the cells were depressurized at a rate of 0.1 bar per second by opening the outlet valve and then vacuuming for 2-3 minutes to remove any excess pressure.

15. Following vacuuming, each cell, including the cap and steel ball, was thoroughly washed using tap water, Zalo (Lilleborg AS), acetone (VWR), and deionized water. Finally, the cells were blow-dried using a high-pressure air gun (Biltema, 15-192).

16. The final step involved transferring the pressure and temperature data obtained from each run to Excel and determining the KHI performance.

Figure 2.5 *SNG bottle, RC-Control Panel box, and compressor unit. The five cells used for testing are on top of the compressor.*

All of the tests were repeated several times due to the stochastic nature of hydrate formation [51, 62]. An example of how a typical graph looks like with this test method and all cells combined is presented below (**Figure 2.6**).

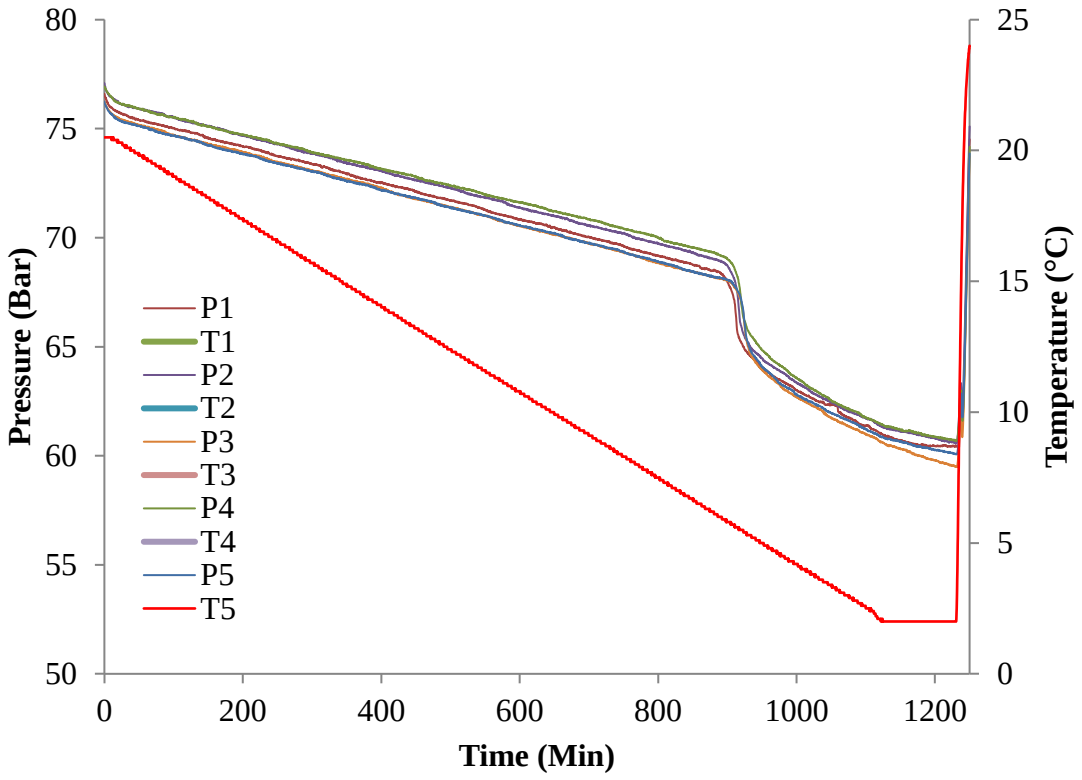

Figure 2.6 *Typical graph of pressure and temperature data obtained by the constant cooling method. The graph displays pressure and temperature versus time. The result in this graph belongs to the new 4x batch 5000 ppm PVAmBu$_2$O with the addition of 5000 ppm nBGE in SNG at 76 bar. The pressure and temperature for each cell are denoted by P and T. The red, thin, decreasing line denotes the temperature curve.*

The pressure in all cells drops at a constant rate from around 76 bar down to approximately 68 bar, at which point the pressure curve starts to deviate from the temperature curve (**Figure 2.6**). The stochastic nature of hydrate formation is not evident in this graph, as all cells have approximately the same temperature values for the first hydrate formation and the most rapid hydrate formation (a further explanation of how of these values are obtained is depicted below in the figure below).

Graphical determination of T_o and T_a values:

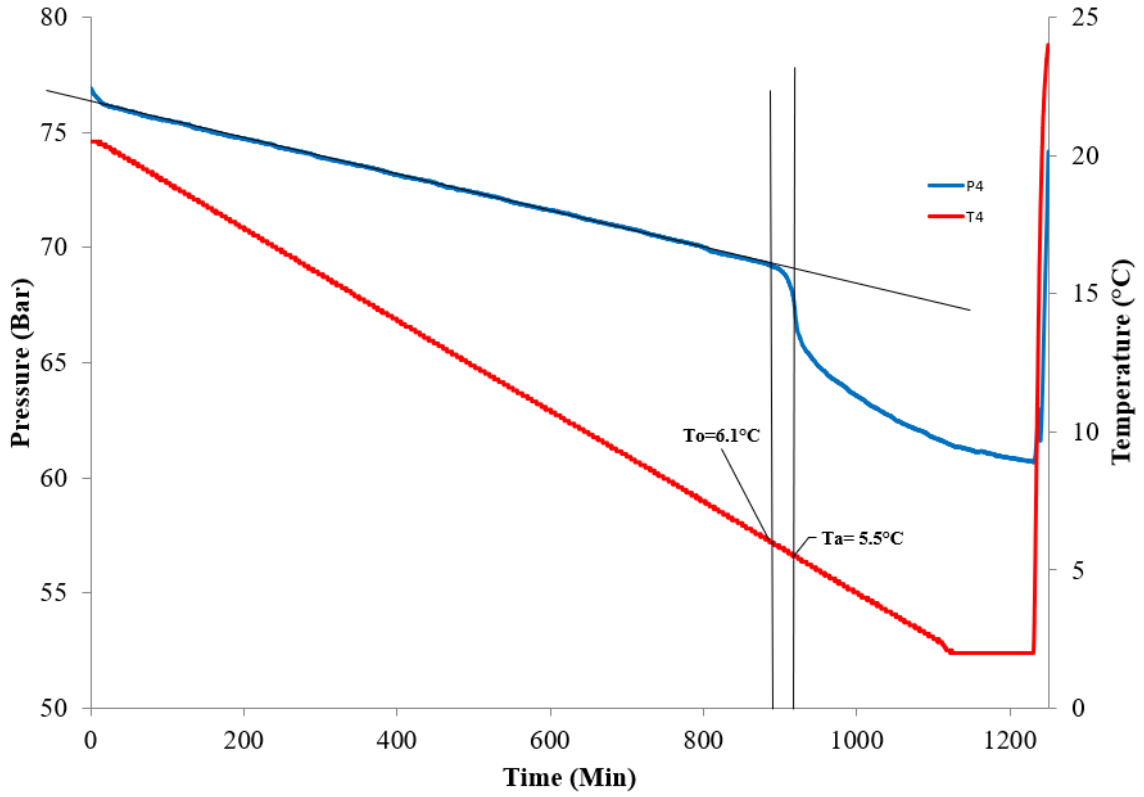

Figure 2.7 *Determination of T_o and T_a values from graph obtained from the constant cooling method with SNG at 76 bar pressure. The pressure and temperature are denoted by P4 and T4.*

The pressure and temperature data obtained from the RC5 were transferred to Excel for a determination of the onset temperature (T_o), and the temperature for the fastest rate of hydrate formation (T_a) from each cell. The onset temperature, T_o, is determined based on the temperature when the pressure starts to deviate from its tangent line, while the temperature, T_a, is determined by the temperature when the pressure has its steepest decline. The values are derived graphically, as illustrated in **Figure 2.7**.

The numerical value obtained by subtracting the T_o value from the T_a values indicates the inhibitor's effectiveness in inhibiting hydrate growth. However, this method is only reliable if the T_o is similar to the T_a and also depends on what the subcooling is at T_o [66].

2.3.1.2 Methane as Test Gas

The slow constant cooling method was also performed in methane gas (supplied by Yara Praxair) on the RC5-2 rig with the same test procedures and cell volumes. A test pressure of 110 bar was used.

2.3.2 Isothermal Test

The isothermal tests were performed in both SNG and methane with the same equipment, test pressure, and test procedure (gas supply, vacuum, etc) as the slow constant cooling method (SCC).

2.3.2.1 SNG as Test Gas at 7 °C

Based on previous experiments, the isothermal temperature for the SNG tests was chosen to be 7 °C [69]. The program for the isothermal test was set up to rock the cells at a start temperature of 20.5 °C, followed by a cool-down period of 1.5 hours to 7 °C. Then, the cells were held rocking at 7 °C for 18 hours before the temperature was increased to 25 °C in a time interval of 20 minutes. The last step involved decreasing the temperature from 25 °C to 20.5 over a few hours. Pressure and temperature data were logged using the same software used for the SCC test, and the t_o (induction time) and t_a (fastest time for hydrate formation) were determined in Excel. A visual example how how such a test looks like with all cells combined is depicted in **Figure 2.8**.

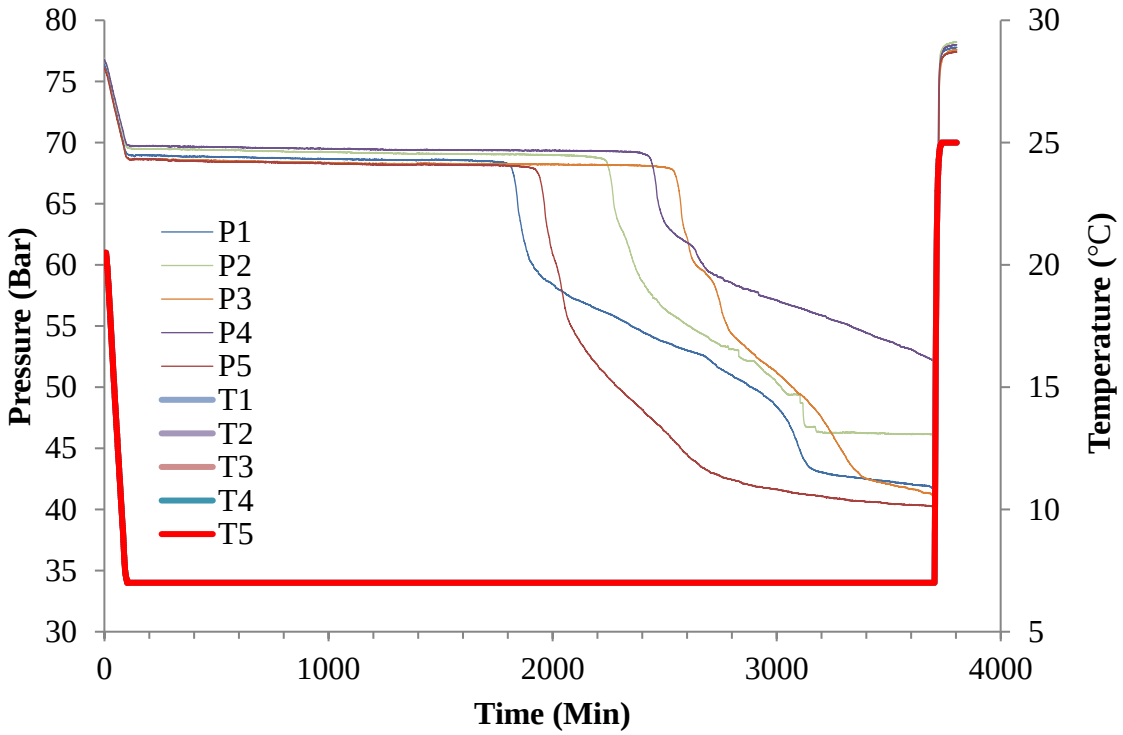

Figure 2.8 *Typical graph of pressure and temperature data obtained by the isothermal method. The result in this graph belongs to the 7 ˚C isothermal test containing 5000 ppm new 4xbatch PVAmBu$_2$O with 5000 ppm nBGE in a 3 wt.% NaCl solution. The pressure and temperature for each cell are denoted by P and T. The red, solid line is the temperature curve.*

The stochastic nature of hydrate formation is clearly evident in this figure (**Figure 2.8**), as the cells form hydrates at different times, despite having the same chemical composition. Cell 1 (blue line) was the first of the five cells to form hydrates as the pressure dropped rapidly at approximately 1800 minutes. The other cells followed in the order: cell 5 (brown), cell 2 (green), cell 3 (orange) and cell 4 (purple). A long delay of hydrate formation was observed as the pressure curve was horizontal until 1800 minutes.

An example of how to derive the t_o and t_a values graphically is presented in **Figure 2.9**.

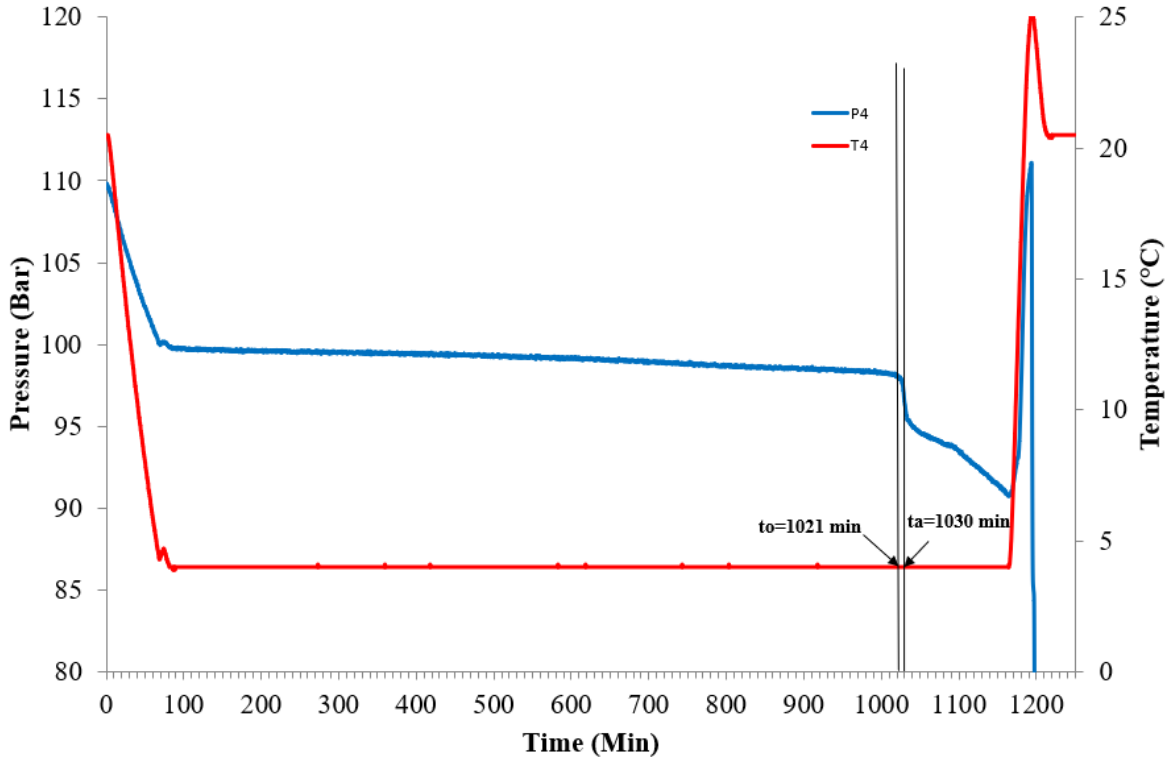

Figure 2.9 *Determination of t_o and t_a values from graph obtained from the isothermal method with methane at 110 bar and 4 °C. The pressure and temperature are denoted by P4 and T4.*

2.3.2.2 Methane as Test Gas at 4 °C

The chosen isothermal temperature for the methane test was 4 °C, based on previous experiments [72]. The set-up for the test program was the same as for the SNG isothermal test with the only difference being that the temperature was 4 °C instead of 7 °C. The determination of the t_o and t_a values followed the same procedure as for SNG.

3 Results

This chapter contains the results obtained with the constant cooling method and the isothermal method. The chapter is divided into sections based on each chemical class to provide an easier overview of the results.

Deionized water (dH_2O) and PVCap were tested for comparison with each chemical class. Synergists additions of iBGE, nBGEn, DPBGE and 3 wt.% NaCl was also included. The number of parallels (n) per test run varied from two to five. As previously mentioned, all tests were repeated several times due to the stochastic nature of hydrate formation. The focus of the values in each table will be centered around the onset hydrate formation temperature (T_o) as this parameter reflects the temperature at which the first hydrate particles start to form and can thus be regarded as the primary parameter for assessing the performance of the KHI. A low T_o value generally correlates to high KHI performance [48]. The primary focus for the isothermal tests will be the induction time, t_o, as it can be regarded as the analog to the T_o in the SCC tests.

3.1 Polyvinyl Amine Oxides

Note that all samples labeled $PVAmBu_2O$ in the tables/figures were synthesized with low polymer molecular weight unless stated otherwise.

3.1.1 Results from the Various Syntheses

The pentyl version was synthesized, but the resulting product was insoluble and could not be tested on the RC5 rig. Additionally, attempts to synthesize other versions of the polyvinyl amine oxides, such as the $PVAmiBu_2O$ or to substitute sodium hydroxide with $NaHCO_3$ or Na_2CO_3, as well as the synthesis of N-isopropyl-3-isopropylamino-propanamide (SAM3i) synthesis did not yield any product.

A significant discrepancy in the synthesis process was that the $PVAmBu_2O$ polymer did not behave consistently after each time it was synthesized. Occasionally, three layers were observed instead of two in the separating funnel and the amount of product yield varied each time. The polymer also varied from being solid or liquid after rotary evaporation. Moreover, the medium molecular weight synthesis resulted in two separate products instead of one.

3.1.2 Slow Constant Cooling Test Results in SNG

The SCC experiments were performed with a cell volume of 20 mL and a test pressure of 76 bar.

Table 3.1 *SCC test results in SNG for polyvinyl amine oxide samples. The polymer and synergist concentrations were variable. The average temperature for the onset of hydrate formation is represented by the T_o average values, while the average temperature for the fastest hydrate growth is represented by the T_a average values. The T_o-T_a values indicate the polymer`s inhibitor capacity.*

Polymer Name + Additive	**Test concentration [ppm]**	**(T_o)Avg [˚C]**	**(T_a)Avg [˚C]**	**(T_o-T_a)Avg [˚C]**
dH_2O (Deionized water)	n/a	16.8	16.4	0.4
PVCap powder	2500	9.7	9.3	0.4
$PVAmBu_2O$ (Old solution from Cecilie*)	2500	9.3	8.9	0.4
$PVAmBu_2O$ (from Cecilie) + iBGE	2500 + 5000	8.1	7.6	0.5
$PVAmBu_2O$ (from Cecilie) + iBGE	2500 + 10 000	8.5	8.0	0.5
Solid $PVAmBu_2O$	2500	15.6	14.7	0.9
Liquid $PVAmBu_2O$	2500	11.7	11.3	0.4
Liquid $PVAmBu_2O$ + nBGE	2500 + 5000	7.4	6.5	0.9
Liquid $PVAmBu_2O$ + DPBGE	2500 + 5000	10.0	9.7	0.3
Low M_w $PVAmBu_2O$	2500	11.8	11.2	0.6
Low M_w $PVAmBu_2O$ + iBGE	2500 + 5000	10.8	10.3	0.5
High M_w $PVAmBu_2O$	2500	13.5	12.9	0.6
High M_w $PVAmBu_2O$ + nBGE	2500 + 5000	13.0	12.5	0.6
Low M_w $PVAmPr_2O$	2500	13.8	13.4	0.4
Medium M_w $PVAmBu_2O$ I	2500	12.8	12.3	0.5
Medium M_w $PVAmBu_2O$ II	2500	13.9	13.4	0.5
4x batch $PVAmBu_2O$	10 000	8.6	8.0	0.6
$PVAmBu_2O$ w/acetonitrile	2500	16.0	15.0	1.0
PVAmBu2 w/acetonitrile (quat. I)	2500	17.1	16.5	0.5
$PVAmBu_2O$ Cecilies method	2500	13.3	12.8	0.5
Michael addition (Lupamin vac down split product)	2500	15.9	15.2	0.7
$PVAmBu_3Br$ quat. w/acetonitrile	2500	16.2	15.2	0.9
PVAmBuO (mono butylated)	2500	9.5	8.8	0.7
Lupamin Vac down	2500	13.0	12.6	0.4
4x batch $PVAmBu_2O$	5000	8.7	8.1	0.6
4x batch $PVAmBu_2O$	2500	8.0	7.3	0.7
4x batch $PVAmBu_2O$ + 3 wt.%NaCl	2500	6.0	4.9	1.0
New 4x batch $PVAmBu_2O$	2500	7.1	6.3	0.8
New 4x batch $PVAmBu_2O$	5000	6.2	5.5	0.7

New 4x batch PVAmBu$_2$O +nBGE	5000 + 5000	5.9	5.5	0.4
PVCap+nBGE	5000 + 5000	5.2	2.4	2.8

*Cecilie was a previous bachelor's student at UiS.

Table 3.1 summarizes the results from the SCC tests in SNG for polyvinyl amine oxides. A general observation was that the T_o and T_a values for all samples followed the same trend with the T_a having a lower value than the T_o. Another observation was that the synthesized products performed better than deionized water.

The polyvinyl dibutyl amine oxide (PVAmBu$_2$O) samples at a concentration of 2500 ppm had a wide range in the average onset temperature, ranging from 7.1 to 15.6 ˚C, indicating that the synthesis did not yield a consistent product each time. However, it seems that the performance improved with each synthesis, as the most recent product (new 4x batch PVAmBu$_2$O) had an average onset temperature of 7.1 °C, compared to 11.8 °C for the oldest attempt.

An observed trend was that the molecular weight impacted the performance of the KHI. This was observed in the PVAmBu$_2$O samples with a concentration of 2500 ppm. The sample with low molecular weight had an average onset temperature (T_o) of 11.8 ˚C. As the molecular weights increased, the average T_o also increased. This observation indicates that a low molecular weight results in improved performance.

A consistent trend between polymer concentration and performance could not be observed. The oldest of the quadrupled batches of PVAmBu$_2$O displayed a trend where the average onset temperature increased with increasing polymer concentration, from 8.0 ˚C at 2500 ppm to 8.6 ˚C at 10 000 ppm. This may indicate that a higher polymer dose leads to poorer performance. The opposite trend was observed in the most recent quadrupled batch, where the average onset temperature decreased as the polymer concentration increased which indicated that the performance increased with a higher polymer dose.

Another visible trend was that the addition of synergists improved the KHI performance. A consistent trend was observed with the synergists iBGE, nBGE, and DPBGE where the average onset temperature decreased when the synergist was added at a concentration of 5000 ppm. The new 4x batch PVAmBu$_2$O combined with nBGE at a concentration of 5000+5000 ppm had a similar performance to PVCap with added nBGE at the same concentrations, as the average T_o values were 5.9 and 5.2 ˚C, respectively. Additionally, NaCl was also found to be a synergist as the average T_o value decreased from 8.0 to 6.0 ˚C post salt addition.

The changes made to the PVAmBu$_2$O synthesis did not improve its performance, as the average onset temperature increased significantly. For example, substituting the solvent isobutyronitrile to acetonitrile or subjecting the polymer Lupamin 1595 to rotary evaporation prior to performing the other synthesis steps, did not yield better results in the form of lower average T_o values. An interesting finding is that the oxidized acetonitrile sample had an average onset temperature of 16.0 ˚C, similar to deionized water, while the non-oxidized sample performed even worse than water. Additionally, alternating the number of butyl groups also had an impact on the performance, as the tributylated alternative had a poorer performance than the dibutylated alternatives.

3.1.3 Impact of Molecular Weight on KHI Performance in SNG

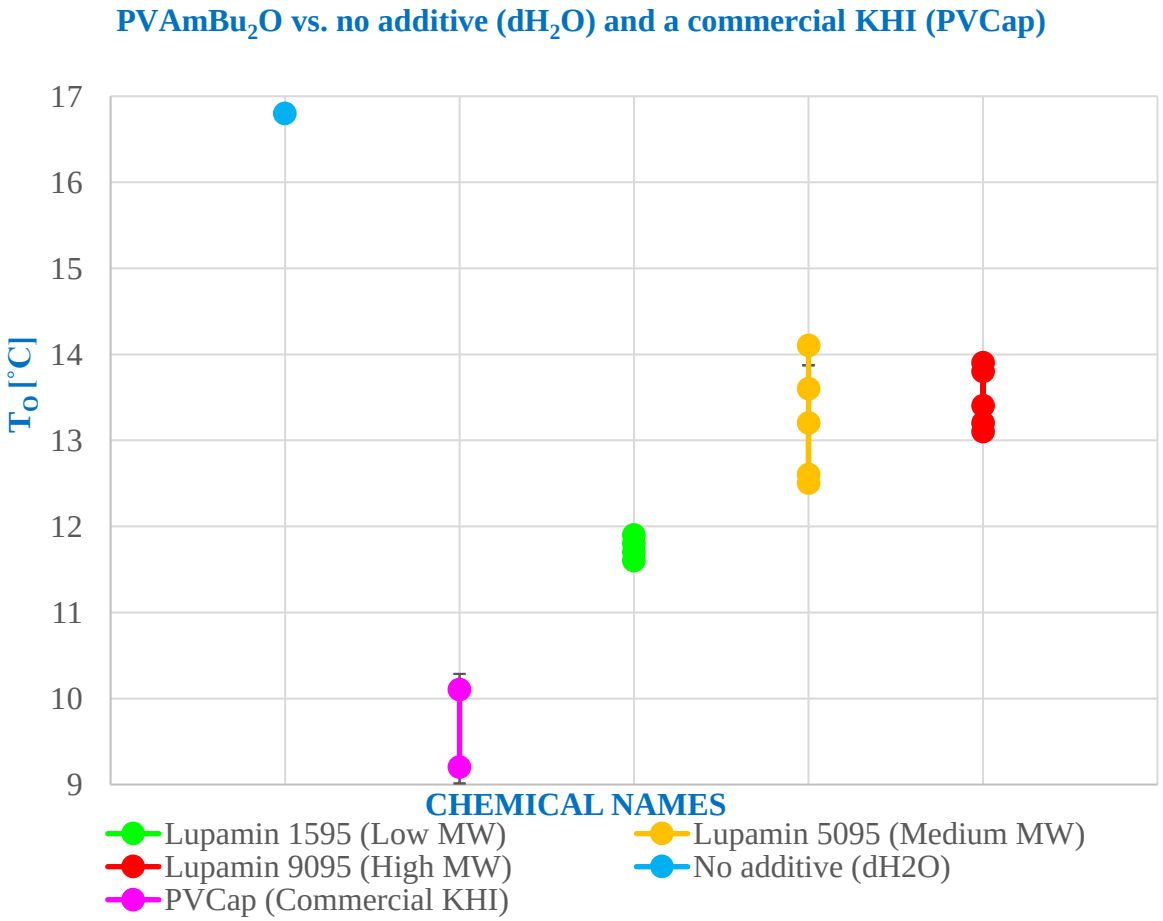

Figure 3.1 *SCC tests with varied polymer molecular weights in SNG. The polymer concentration was 2500 ppm, and the cell volume was 20 mL. The reported T_o values are based on parallel runs and not averages. The T_o values from the medium molecular weight are a combination of the medium molecular weight samples from* ***Table 3.1****.*

Synthesizing the PVAmBu$_2$O with different molecular weights impacted the polymer's performance (**Figure 3.1**), as the T_o increased with increasing molecular weight. The blue dot represents deionized water (dH$_2$O) as a worst-case scenario, whereas the purple dots represent PVCap as the desired T_o value.

The low molecular weight alternative had a T_o of around 11.5-12 ˚C and was slightly worse than PVCap (9.5 ˚C). The stochastic nature of hydrate formation was more evident in the medium molecular weight sample as a larger spread in the T_o values was observed. The high and medium molecular weight samples had a T_o of around 13 to 14 ˚C. It seemed that the medium molecular weight alternative yielded the worst performance. However, the general trend indicated that lower polymer molecular weight was linked to better performance.

3.1.4 Slow Constant Cooling Test Results in Methane

Table 3.2 *SCC test results in methane for the polyvinyl dibutyl amine oxide samples. The polymer and synergist concentrations were variable. The average temperature for the onset of hydrate formation is represented by the T_o average values, while the average temperature for the fastest hydrate growth is represented by the T_a average values. The T_o-T_a values indicate the polymer`s inhibitor capacity.*

Polymer Name + Additive	**Test Concentration [ppm]**	**(T_o)Avg [˚C]**	**(T_a)Avg [˚C]**	**(T_o-T_a) Avg [˚C]**
4x batch PVAmBu$_2$O	2500	3.1	3.0	0.1
4x batch PVAmBu$_2$O + nBGE	2500 + 5000	3.3	3.1	0.1
dH$_2$O	n/a	11.9	11.8	0.1
New batch PVAmBu$_2$O	2500	3.7	3.4	0.2
New batch PVAmBu$_2$O + iBGE	2500 + 5000	4.5	4.4	0.2
dH$_2$O + iBGE	n/a + 5000	12.1	11.8	0.3
4x batch PVAmBu$_2$O	5000	6.7	6.1	0.6
New 4x batch PVAmBu$_2$O	2500	4.2	3.9	0.3
New 4x batch PVAmBu$_2$O	5000	3.0	2.2	0.9
New 4x batch PVAmBu$_2$O + 3wt.%NaCl	5000	2.9	2.0	0.9
New 4x batch PVAmBu$_2$O + 3wt.%NaCl	2500	2.5	2.0	0.5
New 4x batch PVAmBu$_2$O +nBGE +3wt.%NaCl	5000 + 5000	2.6	2.0	0.6
PVCap+nBGE	5000 + 5000	6.1	4.9	1.2
PVCap	5000	5.7	5.3	0.4
PVCap*	2500	7.8	7.4	0.4

*Unpublished data

Table 3.2 summarizes the results from SCC tests in methane. The average T_o and T_a values generally follow the same trend with the T_a having a lower value than the T_o. All polymers performed better than deionized water.

The various batches of PVAmBu_2O at 2500 ppm without additives, displayed significantly better performance than PVCap at the same concentration. Depending on the sample, the average onset temperature of the PVAmBu_2O was (or almost) half that of PVCap.

A clear pattern of concentration-dependent performance was not observed. The performance of the oldest 4x batch of PVAmBu_2O became worse as the concentration increased, while the most recent 4x batch displayed the opposite behavior where an increase in concentration resulted in better performance. Moreover, the most recent quadrupled batch outperformed PVCap at a 5000 ppm concentration as the average onset temperature was lower.

The addition of synergists had different effects on the performance. Adding nBGE and iBGE did not improve the performance as the T_o average increased. However, using salt as an additive, improved the performance as the average onset temperature decreased. Additionally, when the polymer was added with both nBGE and salt at a concentration of 5000 ppm, the performance increased suggesting that nBGE had a small synergistic effect at that concentration as the nBGE addition was the only non-constant variable.

3.1.5 Impact of Test Gas on KHI Performance

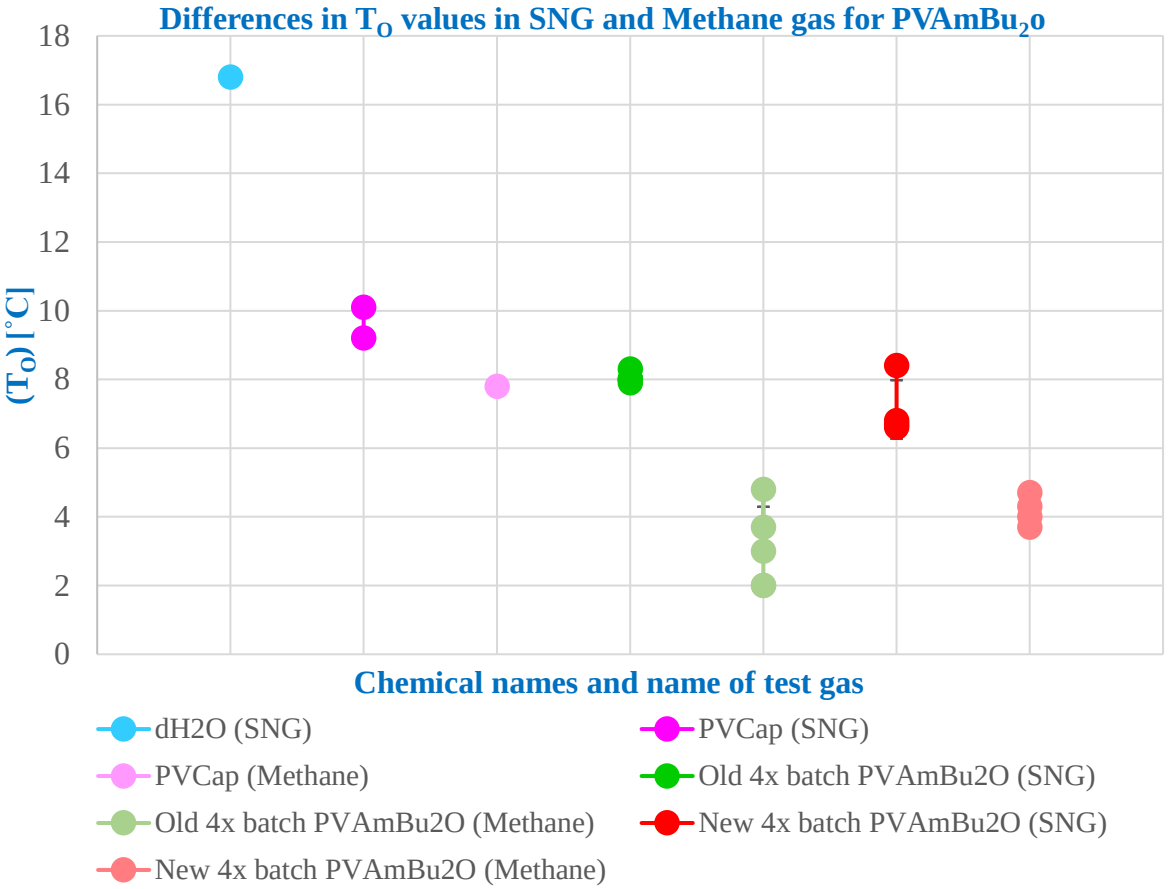

Figure 3.2 *Comparison of performance in SNG and methane for the PVAmBu$_2$O polymers. The polymer concentration was 2500 ppm and the cell volume was 20 mL. Note: The PVCap data point in methane is derived from unpublished data and represents the average onset temperature not single values like the other samples. SNG samples are represented by bright colors, while methane samples are represented by softer, more diffuse colors.*

Figure 3.2 provides a summary of how the PVAmBu$_2$O polymers performed in SNG and methane. Generally, the performance in methane appeared to be noticeably better compared to SNG. This is evident from the significant decrease in the onset temperature from SNG to methane in both PVAmBu$_2$O samples. An interesting observation is that both sets of the 4x batch polymers outperformed PVCap in both test gases. In SNG, the performance of the PVAmBu$_2$O was slightly better than PVCap. In contrast, the onset temperature of the different PVAmBu$_2$Os decreased significantly in methane compared to PVCap, indicating that the polymers may perform better in methane-dominated systems.

3.1.6 Isothermal Test Results in SNG

The difference between the new and 4x batches of the $PVAmBu_2O$ samples is negligible. They were synthesized in the exact same way, had a similar weight percent, and can therefore be compared.

Table 3.3 *Overview of isothermal tests in SNG. The polymer concentration was variable, and the cell volume was 20 mL for all tests. Each test consisted of five parallels. The average time (in minutes) for the first hydrate formation is represented by the (t_o) average values, while the fastest time for hydrate formation is represented by the (t_a) average values.*

Constant Temp. [˚C]	**Duration [Days]**	**Polymer Name + Additive**	**Test Concentration [ppm]**	**(t_o)Avg [min]**	**(t_a)Avg [min]**
7.0	1	PVCap	5000	93	116
7.0	1	PVCap + nBGE	5000 + 5000	230	297
4.0	1	4x batch $PVAmBu_2O$+nBGE	5000 + 5000	>1200	>1200
4.0	3*	New 4x batch $PVAmBu_2O$ + nBGE + 3wt.%NaCl	5000 + 5000	120	140
7.0	3*	New 4x batch $PVAmBu_2O$ + nBGE + 3wt.%NaCl	5000 + 5000	2192	2232
7.0	1	Old 4xbatch $PVAmBu_2O$ + nBGE	2500 + 5000	99	106
7.0	1	New 4x batch $PVAmBu_2O$ +nBGE +3 wt.%NaCl	2500 + 5000	93	116

*The test duration was expected to be 3 days, but hydrate formation occurred quicker.

A summary of the isothermal tests performed in SNG with temperatures ranging from 4 to 7 ˚C is provided in **Table 3.3**. A general observation is that the average t_o and t_a values follow the same trend for all samples, with the average t_a value being consistently longer than the average t_o value.

The synergist addition had a large impact on the average induction time (t_o) in the isothermal test performed at 4 ˚C. Adding the polymer and nBGE in a 5000+5000 ppm concentration resulted in a prolonged delay in the average induction time (>1200 minutes), while salt addition to the same sample made the average induction time become substantially shorter (120 minutes). This indicates that salt addition does not contribute as a synergist to delay the hydrate formation time.

A noticeable trend observed was that a higher concentration of polymer led to a longer induction time. This was evident in the isothermal tests conducted at 7 ˚C. An example from the table is the comparison of the new 4x batch $PVAmBu_2O$, containing either 5000 or 2500 ppm of polymer and an additional 5000 ppm of nBGE with salt. The 5000 ppm alternative

had a significantly longer average induction time, measuring 2192 minutes (36.5 hours) compared to the 2500 ppm alternative, where the average induction time was 93 minutes. Comparatively, the sample that contained 5000 ppm PVCap with 5000 ppm nBGE addition, only yielded an average induction time of 230 minutes, making the impressive average induction time of 2192 minutes for the 5000 ppm sample even more noteworthy.

In addition, salt addition at 7 ˚C had a small synergistic effect as the average induction was reduced by six minutes.

3.1.6.1 Unusual Behavior in the 7 ˚C Isothermal Test in SNG

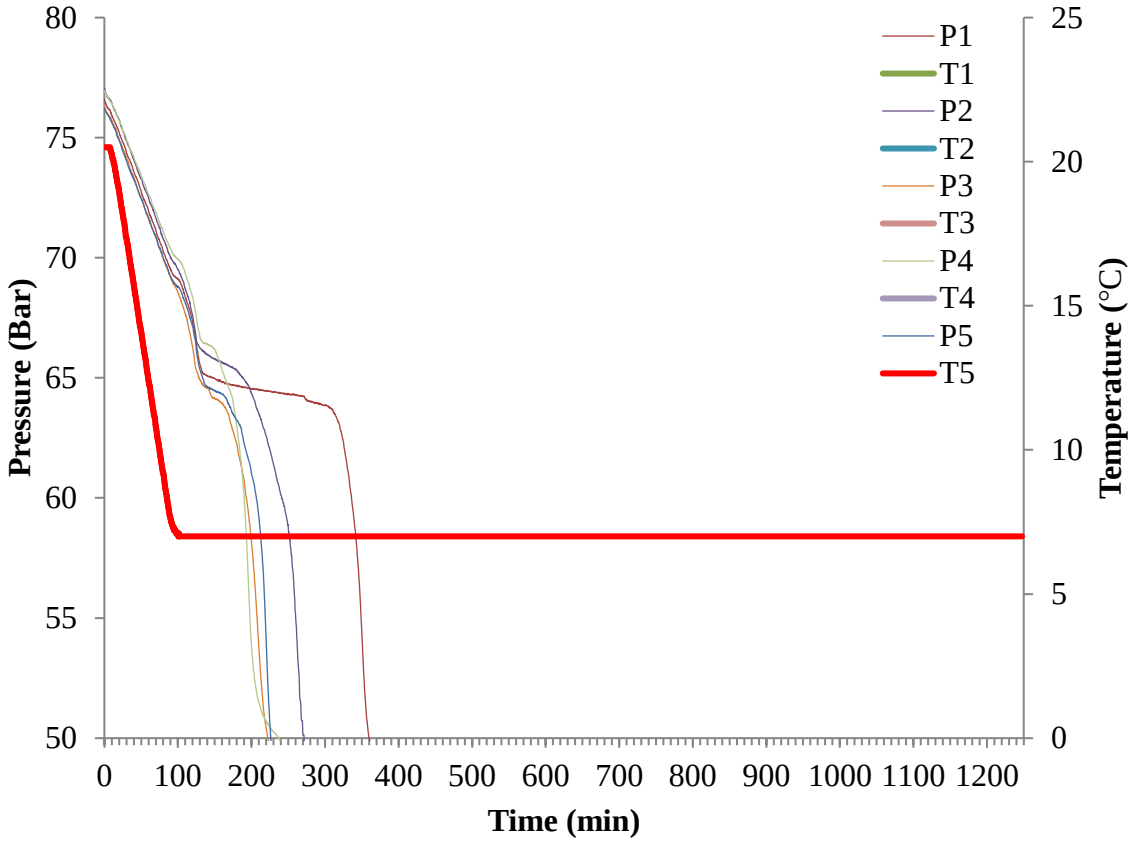

Figure 3.3 *All five cells show a double pressure drop. The sample depicted was the 2500 ppm new 4x batch PVAmBu$_2$O in combination with 5000 ppm nBGE and 3 wt.% NaCl. The test volume was 20 mL for all cells. The pressure and temperature for each cell are denoted by P and T.*

An unusual double pressure drop behavior was observed for each cell (**Figure 3.3**) containing the 2500 ppm new 4x batch PVAmBu$_2$O with 5000 ppm nBGE and 3 wt.% NaCl. A second t_a was observed after the pressure was constant for a while, approximately 1-3 hours after the first t_a. This unusual behavior may indicate the presence of a mixture of different hydrate structures in the sample.

3.1.7 Isothermal Test Results in Methane

Table 3.4 *Overview of isothermal tests in methane. The polymer concentration was variable, and the cell volume was 20 mL for all tests. Each test consisted of five parallels. The average time (in minutes) for the first hydrate formation is represented by the (t_o) average values, while the fastest time for hydrate formation is represented by the (t_a) average values.*

Constant Temp. [˚C]	Duration [Days]	Polymer Name + Additive	Test Concentration [ppm]	(t_o)Avg [min]	(t_a)Avg [min]
7.0	1	4x batch PVAmBu$_2$O + nBGE	5000 + 5000	no drop**	no drop**
4.0	1	4x batch PVAmBu$_2$O + nBGE	5000 + 5000	1068	1079
4.0	1	dH$_2$O	n/a	40	51
4.0	1	PVCap + nBGE	5000 + 5000	70	100
4.0	3*	Old 4x batch PVAmBu$_2$O + nBGE + 3wt.%NaCl	2500 + 5000	51	54
4.0	1	New 4x batch PVAmBu$_2$O + nBGE + 3wt.%NaCl	5000 + 5000	735	748

*The test duration was expected to be 3 days, but hydrate formation occurred quicker.

** “no drop” means that no pressure drop occurred due to hydrate formation.

Table 3.4 summarizes the results of the PVAmBu$_2$O isothermal testing in methane. All samples performed better than deionized water at 4 ˚C. Additionally, the average t_o and t_a values followed the same trend, with the average t_a value being consistently longer than the average t_o value.

No pressure drop was visible in the isothermal test at 7 ˚C, indicating that a larger subcooling was required for hydrate formation to occur.

The addition of 3 wt.% NaCl had an antagonistic effect on the hydrate delay time as the average induction time increased with salt addition. This effect was observed in the samples containing 5000 ppm polymer and 5000 ppm nBGE with salt addition, where the average induction time was 735 minutes (12 hours), compared to 1068 minutes (18 hours) when the polymer and synergist concentrations were the same only without salt addition. However, both of these samples outcompeted PVCap with nBGE at the same concentration, as the average induction time was only 70 minutes for PVCap and nBGE.

An observed trend was that a higher polymer concentration led to a longer induction time. For instance, when using a concentration of 5000 ppm polymer and 5000 ppm nBGE along with salt addition, the average induction time was 735 minutes. In comparison, a polymer concentration of 2500 ppm with the same amount of synergist and salt addition resulted in an average induction time of 51 minutes.

3.2 Poly(2-dialkylamino-2-oxazoline)s

3.2.1 Slow Constant Cooling Test Results in SNG

Table 3.5 *SCC test results in SNG for poly(2-dialkylamino-2-oxazoline)s. The polymer and synergist concentrations were variable, and the cell volume was variable. The average temperature for the onset of hydrate formation is represented by the T_o average values, while the average temperature for the fastest hydrate growth is represented by the T_a average values. The T_o-T_a values indicate the polymer`s inhibitor capacity.*

Polymer Name + Additive	**Test Concentration [ppm]**	**(T_o) Avg [˚C]**	**(T_a) Avg [˚C]**	**(T_o-T_a) Avg [˚C]**	**Test volume [mL]**
Deionized water (dH_2O)	n/a*	16.8	16.4	0.4	**20**
PVCap powder	2500	9.7	9.3	0.4	**20**
SJ192	2500	8.7	7.8	0.9	**20**
SJ192 + iBGE	2500 + 5000	7.3	5.0	2.4	**20**
SJ192 + iBGE	2500 + 10 000	6.8	5.9	0.9	**20**
SJ192 +DPBGE	2500 + 5000	7.5	6.1	1.4	**20**
SJ192 + TiPeAO+iBGE	2500 + 2500 + 10 000	14.7	9.3	5.4	**20**
SJ192 + nBGE	2500 + 5000	7.9	6.1	1.8	**20**
SJ192 + nBGE	2500 + 10 000	7.8	6.0	1.8	**20**
SJ192 + TiPeAO	2500 + 2500	11.5	9.5	2.0	**20**
SJ258	10 000	7.0	5.4	1.7	10
dH2O	n/a*	16.4	16.2	0.2	10
SJ258	5000	7.6	7.1	0.5	10
SJ258	2500	10.1	9.8	0.3	10
SJ258	1000	12.2	12.0	0.2	10
SJ258	2500	9.4	8.9	0.5	**20**
SJ192 + nBGE	2500 +10 000	7.1	6.4	0.7	10
SJ244	10 000	8.9	6.4	2.4	10
SJ244	5000	8.6	7.5	1.1	10
SJ244	2500	10.0	9.5	0.6	10
SJ244	1000	12.4	12.1	0.3	10
SJ268	2500	10.9	10.5	0.4	10
SJ271	2500	11.1	10.3	0.8	10
SJ272	2500	10.1	9.1	1.1	10
SJ274	2500	11.9	11.1	0.7	10
SJ272	5000	11.1	7.9	3.1	10
SJ272	1000	12.3	11.8	0.5	10
SJ258 + iBGE	2500 + 10 000	9.0	8.8	0.2	10
SJ258 + iBGE	5000 + 10 000	9.2	8.6	0.5	10
SJ271	5000	11.4	9.0	2.4	10
SJ272 + iBGE	2500 + 10 000	10.8	10.0	0.8	10
SJ272 + 3wt.%NaCl	2500	11.6	11.4	0.3	10
SJ301	2500	10.9	9.6	1.3	10

SJ258 + iBGE	2500 + 10 000	6.8	6.6	0.2	**20**
SJ301	2500	7.9	7.4	0.5	**20**
SJ258 (old sample)	2500	9.2	8.8	0.4	**20**
SJ244 (old sample)	2500	8.8	8.3	0.5	**20**
SJ301 + 3wt.%NaCl	2500	8.2	7.1	1.1	10
SJ268 + 3wt.%NaCl	2500	10.6	8.4	2.2	10
SJ244 + 3wt.%NaCl	2500	9.9	7.7	2.2	10
SJ268 + TiPeAB**	2500 + 5000	13.8	11.1	2.7	10
SJ244 + TiPeAB**	2500 + 5000	13.1	11.7	1.4	10
PVCap	2500	10.3	9.8	0.5	10

*The meaning of the abbreviation "n/a" is "not applicable."

**TiPeAB is an abbreviation for the synergist “Tetra isopentyl ammonium bromide”.

Table 3.5 summarizes the results of all the SCC tests in SNG for the Poly(2-dialkylamino-2-oxazoline)s. All polymers performed better than deionized water.

The average onset temperature for all polymers tested alone, at a 2500 ppm concentration with a cell volume of 10 mL was approximately 10.0 ˚C. This is similar to the PVCap tested at the same concentration and volume. The performance was also better than deionized water for all polymers.

Three trends related to polymer concentrations were observed. The first and second trends were opposite of each other. The first trend showed that an increase in concentration led to improved performance, as seen in polymers SJ258 and SJ244. For SJ258, the average T_o values at 5000 and 2500 ppm concentrations were 7.6 ˚C and 10.1 ˚C, respectively, while for SJ244, the values were 8.6 ˚C and 10.0 ˚C. The second trend, displayed by the SJ272 and SJ271 polymers, indicated that the performance decreased with higher concentrations. The third trend was that the poorest performance was observed with a polymer concentration of 1000 ppm at an average onset temperature of approximately 12 ˚C.

A noticeable pattern was observed where the performance increased with increasing cell volume. The trend can be seen in the SJ258 and SJ301 polymers at 2500 ppm. Taking the SJ258 as an example, a 10 mL sample yielded an average onset temperature of 10.1 ˚C, compared to 9.4 ˚C at 20 mL. Similarly, PVCap at the same concentration also exhibited this behavior.

Another trend was that synergist addition primarily enhanced the polymers' KHI performance. The addition of iBGE and nBGE provided synergistic effects, leading to a decrease in the average onset temperature. The optimal dose was 10 000 ppm synergist along with a 2500

ppm polymer concentration at a 10 mL cell volume. However, the polymer SJ258 displayed a trend where the iBGE addition resulted in a synergistic effect at a polymer concentration of 2500 ppm and an antagonistic effect at a polymer concentration of 5000 ppm.

Furthermore, NaCl and DPBGE additions also contributed to increased performance. An exception was the SJ272 polymer where the performance became worse as salt was added. In addition, the additives TiPeAO and TiPeAB displayed an antagonistic effect when introduced with the polymers.

An unexpected observation was the poor KHI performance observed when the polymer was dosed with two synergists. For instance, in the case of polymer SJ192, synergism was observed when iBGE was added alone, while antagonism was observed when the TiPeAB was added alone with the polymer. However, combining these additives resulted in a substantial increase in the average onset temperature, which increased to 14.7 ˚C. This result was almost as bad as no additive, as the average T_o of deionized water was 16.8 ˚C.

3.2.2 Impact of Solvent Synergist Addition and Variable Cell Volume on KHI Performance in SNG

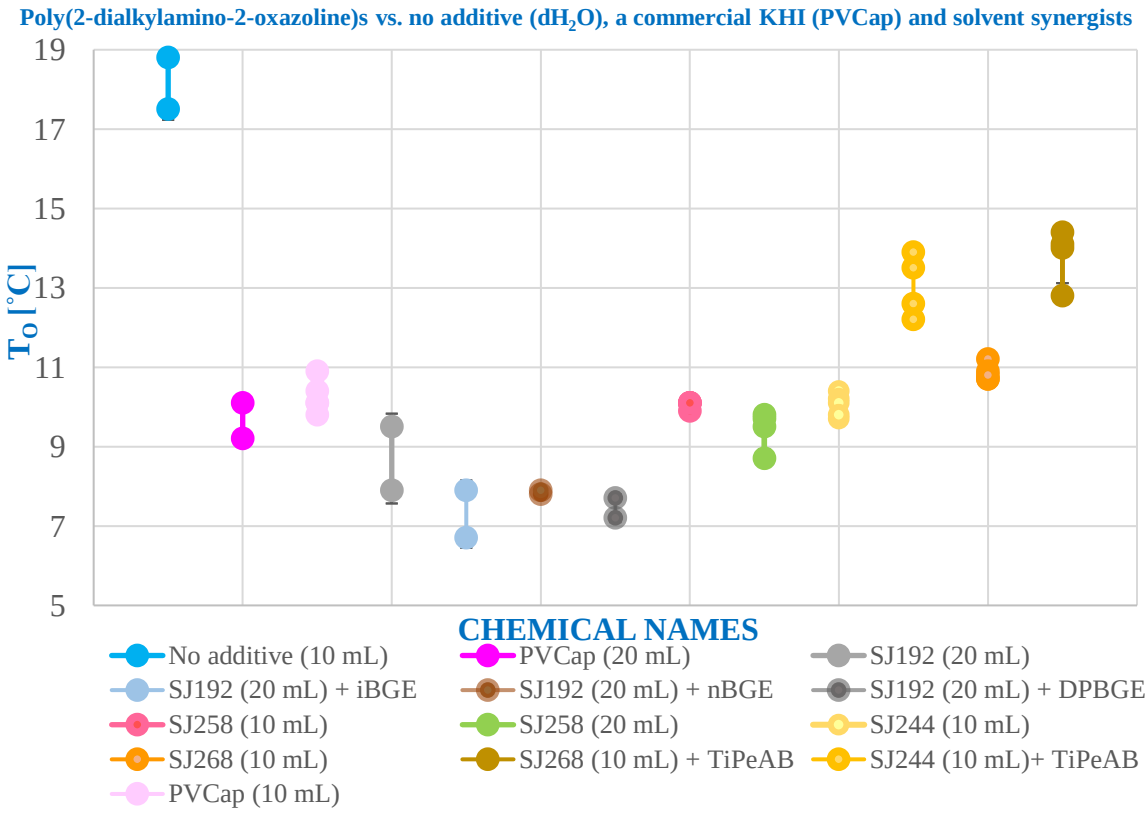

Figure 3.4 *SCC test results for poly(2-dialkylamino-2-oxazoline)s in SNG with various synergist additions. The polymer concentration was 2500 ppm, and the synergist addition was 5000 ppm for all tests. The cell volume was variable.*

The impact of the cell volume on the polymers' performance was evident (**Figure 3.4**). PVCap and SJ258 showed that the 20 mL (purple and green) sample had a slightly lower onset temperature compared to the 10 mL samples (pink and red). This finding suggests that the best performance is achieved with a 20 mL aqueous cell volume.

Additionally, the addition of iBGE (light blue), nBGE (brown), and DPBGE (black) to the SJ192 polymer (gray) increased the performance as the onset temperature decreased, and the best synergistic effect was obtained with iBGE addition. However, an antagonistic effect was observed with the addition of the synergist TiPeAB for the SJ268 (dark yellow) and SJ244 (light brown) samples as the onset temperature was elevated compared to the samples with no additive.

3.2.3 Impact of NaCl Addition on KHI Performance in SNG

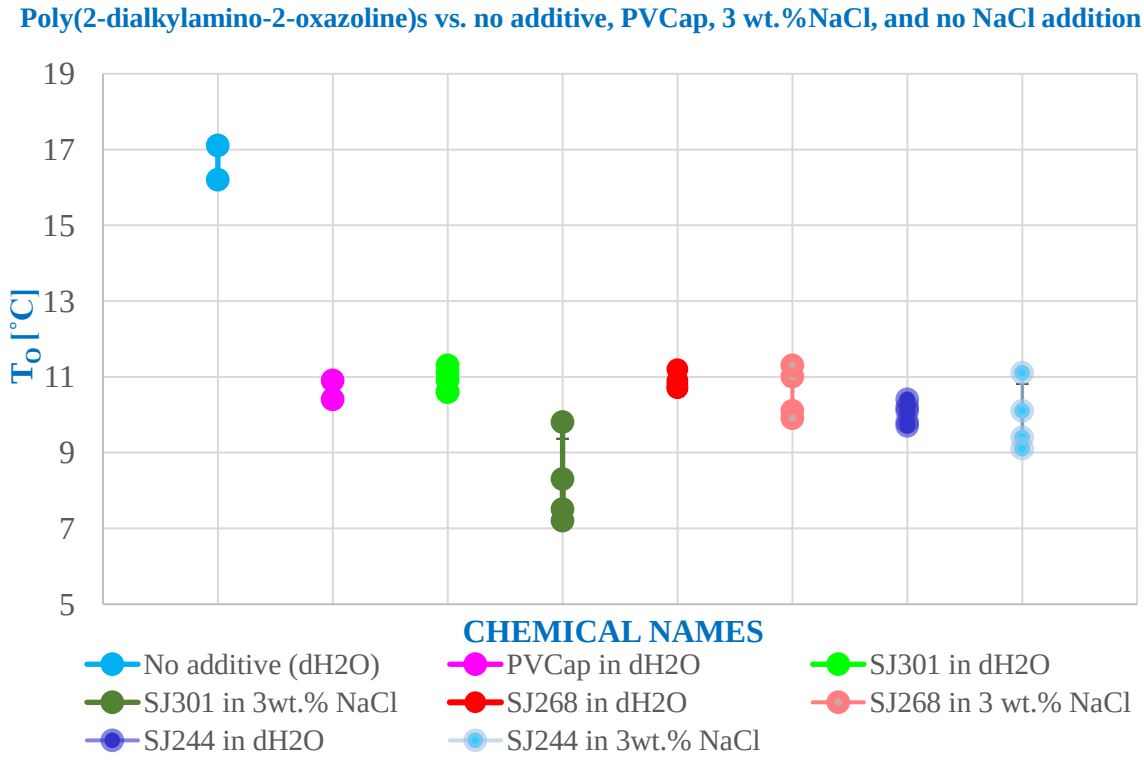

Figure 3.5 *Impact of NaCl addition on T_o values. The polymer concentration for all tests was 2500 ppm, and the cell volume was 10 mL.*

Prior to salt addition, the polymers exhibited similar performance to PVCap at the same concentration (**Figure 3.5**). However, as salt was added to the polymers, the performance increased, visible by the decrease in the onset temperature. The stochastic nature of hydrate formation was more evident in the salt-addition samples, as the T_o values diverged more.

3.2.4 Slow Constant Cooling Test Results in Methane

Table 3.6 *SCC test results in methane for poly(2-dialkylamino-2-oxazoline)s. The polymer and synergist concentrations were variable, as was the cell volume. The average temperature for the onset of hydrate formation is represented by the T_o average values, while the average temperature for the fastest hydrate growth is represented by the T_a average values. The T_o-T_a values indicate the polymer's inhibitor capacity.*

Polymer Name+ Additive	Test Concentration [ppm]	(T_o) Avg [˚C]	(T_a) Avg [˚C]	(T_o-T_a) Avg [˚C]	Test Volume [mL]
SJ244	2500	7.8	7.3	0.5	10
SJ258	2500	7.7	7.5	0.2	10
SJ271	2500	8.6	8.0	0.6	10
SJ258 + iBGE	1000 + 10 000	10.2	9.9	0.3	10
SJ258 + iBGE	5000 + 10 000	9.0	8.4	0.6	10
SJ258 + iBGE	2500 + 10 000	8.5	8.4	0.1	10
SJ272+iBGE	2500 + 10 000	9.5	9.0	0.6	10
SJ258	5000	8.2	7.0	1.2	10
SJ272+ 3 wt.% NaCl	2500	8.4	7.6	0.8	10
SJ301	2500	8.6	7.6	1.0	10
SJ301	5000	9.4	7.5	1.9	10
SJ272	2500	8.8	7.9	0.9	10
PVCap	2500	8.0	7.4	0.6	10
PVCap+nBGE	5000 + 5000	6.1	4.9	1.2	**20**
PVCap	5000	5.7	5.3	0.4	**20**
PVCap*	2500	7.8	7.4	0.4	**20**

*Unpublished data.

Table 3.6 summarizes the results for all the SCC tests in methane for the poly(2-dialkylamino-2-oxazoline)s.

The average onset temperature for all polymers at a concentration of 2500 ppm and 10 mL aqueous volume was around 8.0 ˚C, which is comparable to PVCap at the same volume and concentration.

There was a noticeable trend indicating that performance deteriorated with higher concentrations. This trend was evident for the SJ258 and SJ301 polymers, as the average onset temperatures were higher at 5000 ppm than at 2500 ppm.

The addition of iBGE had an antagonistic effect on the polymers' performance, which was displayed in the SJ258 and SJ272 polymers. Likewise, the nBGE was also not a synergist for PVCap as the performance became worse. However, the addition of 3 wt.% NaCl increased the performance of the SJ272 polymer.

3.2.5 Impact of Test Gas on KHI Performance

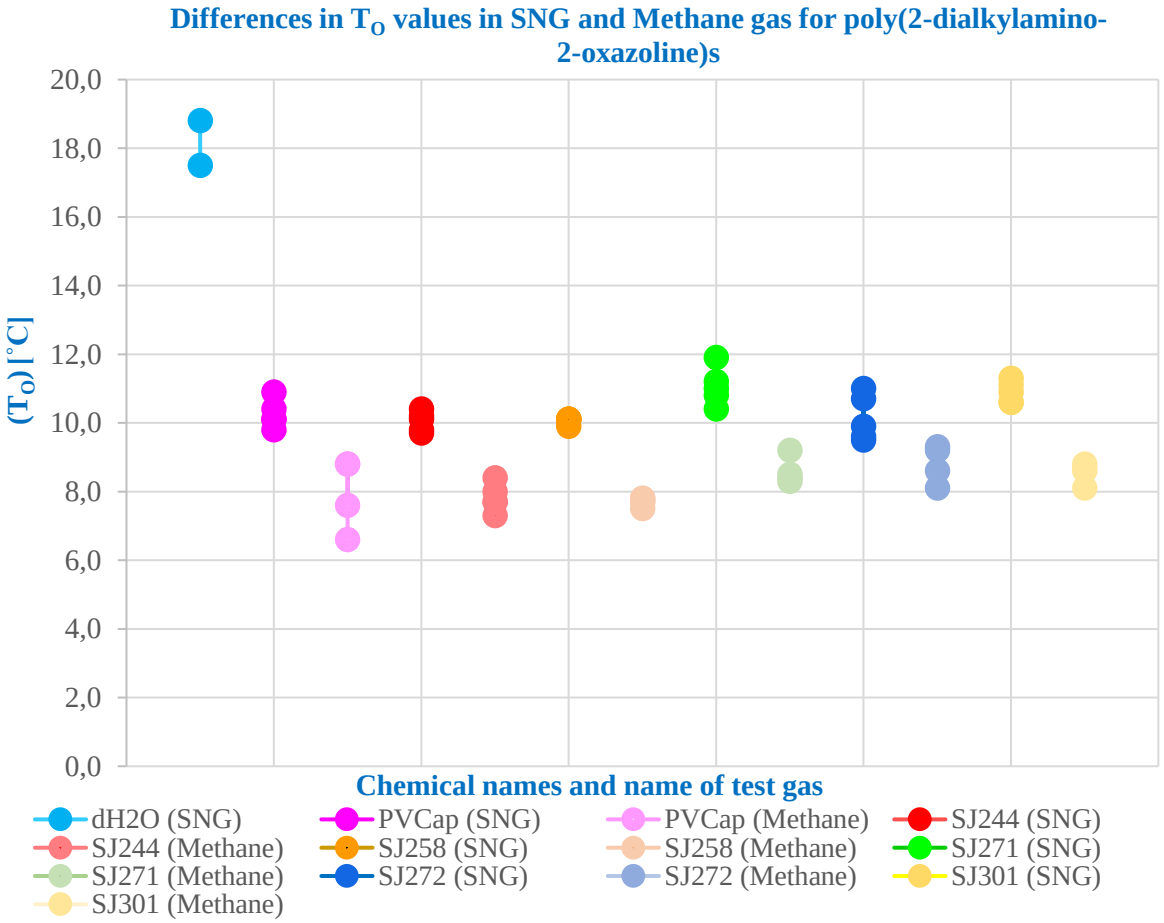

Figure 3.6 *Performance comparison in SNG and methane for the poly(2-dialkylamino-2-oxazoline)s. All polymer concentrations were 2500 ppm, and the cell volume was 10 mL. The SNG samples are represented by bright colors, while the methane samples are represented by softer, more diffuse colors.*

Figure 3.6 presents an overview of the polymer's performance in SNG and methane. A noticeable trend was that the polymers seemed to perform better in methane than in SNG, as the average onset temperature decreased further in methane compared to SNG. The performance in SNG for all polymers was comparable to PVCap's, as they had approximately the same onset temperature. However, the PVCap sample in methane presented a clear, stochastic behavior as the individual T_o values were spread apart, which made it more difficult to compare the performance of the polymers with PVCap. However, in general, the polymers' performance in methane was also similar to that of PVCap.

4 Discussion

This chapter interprets the results from the syntheses and the performance testing, discusses the results' implications and limitations, and compares them to relevant literature data.

4.1 Polyvinyl Amine Oxides

The following subchapters are dedicated to the observable trends and important findings from the synthesis of the polyvinyl amine oxides, the SCC and isothermal tests, and how these results relate to previous work.

4.1.1 Synthesis Discrepancies

The different synthesized products showed a common trend: the ones with bromo-alkanes exhibited the highest performance (**Table 3.1**). Adding butyl bromide in the first synthesis step resulted in the incorporation of two butyl groups, which boosted the performance of the polyvinyl amine oxides. According to KHI theory, the most effective groups for hydrate inhibition are butyl or pentyl groups [41]. This theory was supported by the performance of the butylated polymers synthesized in this thesis. The results from the propylated version further confirm this theory, as the average onset temperature was very poor and similar to having no additive. A surprising result was encountered when the pentyl version was synthesized, as it was insoluble and could not be tested for its performance.

The performance of the 2500 ppm PVAmBu_2O varied significantly each time it was synthesized (**Table 3.1**), leading to contradictory results in **Figure 3.1** and **Figure 3.2**. Figure 3.1 indicated that the performance of the polyvinyl dibutyl amine oxides was not better than PVCap, while Figure 3.2 suggested the opposite. However, since the average onset temperature decreased progressively after each synthesis, it is clear that the synthesis process needs refinement to achieve consistent and trustworthy results.

Another trend was that the performance became worse if the solvent was substituted with acetonitrile instead of isobutyronitrile. A possible explanation may be related to the water solubility of these solvents. The acetonitrile is miscible in water while isobutyronitrile is only slightly miscible in water (3 g/L) [73, 74]. The different water solubilities may play a role in the reaction kinetics and chemical availability.

The N-isopropyl-3-isopropylamino-propanamide (SAM3i) synthesis did not work and the reason behind it may be related to the branching of the molecule [23].

Another modification that did not work was the PVAmiBu$_2$O synthesis. An NMR was taken after the rotary-evaporation step, but the NMR graph did not show any butyl groups, only the presence of iPrCN, indicating that the isobutyl bromide did not incorporate into the polymer. The mechanism of why this occurred is unknown.

The sodium hydroxide was also substituted with $NaHCO_3$ and Na_2CO_3 in two different versions of the "standard" PVAmBu$_2$O synthesis explained in the method section of this thesis. Both of the syntheses did not yield any product. In the case of the $NaHCO_3$ addition, the base may have been too weak to contribute to the reaction compared to the strong base of sodium hydroxide [75]. The mechanism of why the Na_2CO_3 addition did not work is unknown.

The PVAmBu$_3$Br synthesis with acetonitrile yielded an average onset temperature of 16.2 ˚C which is as poor as no additive (deionized water). The reason for the poor performance may be due to the lack of an oxygen atom in the structure as the oxygen atom contributes to increased hydrogen bonding (as reported in the introduction section), or it might have to do with the acetonitrile being the solvent. The interaction of three butyl groups with the hydrate surface, instead of two is apparently insufficient to slow down the hydrate growth as the role of the oxygen atom also plays a significant role in hydrate inhibition. The ^{1}H NMR spectrum presented in **Appendix A**, **Figure 7.1**, provided confirmation of the poor performance, as the graph was very messy, indicating the challenges of obtaining a pure product. The ChemDraw prediction (**Appendix A**, **Figure 7.2**) is also not in line with what was observed in the ^{1}H NMR graph, giving further confirmation of the poor performance.

The addition of only one butyl group (monobutylated PVAmBu$_2$O, **Table 3.1**) made the performance slightly worse as the average onset temperature was 9.5 ˚C compared to 8.0 ˚C which indicates that the presence of two butyl groups is evident to obtain a good KHI performance.

Furthermore, the ^{1}H NMR spectrum of the polyvinyl dibutyl amine (PVAmBu$_2$) in DMSO (**Appendix B**, **Figure 7.3**) displayed a distinct separation of peaks, indicating a pure product. The triplet peak at 3.25 ppm is likely attributed to the two butyl-CH_2-methylene groups on the nitrogen atoms. The peak at 2.85 ppm may correspond to the CH backbone. These findings align with the prediction from ChemDraw (**Appendix B**, **Figure 7.4**), where the CH backbone (linked to nitrogen) and methylene groups are anticipated to occur at the same frequency.

4.1.2 Molecular Weight-Dependent KHI Performance in SNG

Synthesizing the PVAmBu$_2$O with a low molecular weight resulted in an increase in KHI performance (**Table 3.1** and **Figure 3.1**). One potential explanation for the observed trend could be related to the ratio between the surface area of the KHI and its hydrodynamic volume. Maximizing this ratio results in a larger hydration volume, allowing for greater interaction between the KHI and the water and gas molecules that make up the clathrate. As the polymer chain length decreases, the surface area to volume ratio increases. Therefore, a lower molecular weight polymer will exhibit an increased KHI performance due to its larger surface area to volume ratio compared to polymers that have medium or high molecular weighs [31]. Chua et al. reached a similar conclusion using the constant cooling method, where low molecular weight polymers of poly(N-isopropyl acrylamide)s (PNIPAMs) and poly(N-vinyl isobutyramide) (PNVIBAs) demonstrated better KHI performance than the high molecular weight alternatives of the same polymers [76].

However, the low molecular weight PVAmBu$_2$O did not outperform PVCap. The reason is not likely attributed to the polymer molecular weight as they both had the same polymer molecular weight of 10 000 g/mol. However, the answer may lie in the distribution of molecular weight as this is reported to affect the performance of the KHI. A bimodal distribution is reported to yield the best performance. The optimal polymer configuration involves a minor portion with high molecular weight and the majority with low molecular weight [77].

Additionally, the medium molecular weight option appeared to display a larger stochastic nature than the other alternatives, and its performance seemed to be worse than the high molecular weight option (**Figure 3.1**). The reason for the poor performance could be attributed to the synthesis process, which resulted in the production of two different products instead of one (unlike the low and high molecular weight options). Both synthesized products were combined in the figure to increase the sample number (n=5) making it comparable to the sample numbers (n=4 and n=5) of the low molecular and high molecular weight alternatives, respectively.

4.1.3 Concentration Effects on KHI Performance in SNG and Methane

The different batches of PVAmBu$_2$O exhibited different behaviors at different concentrations in SNG with the constant cooling method (**Table 3.1**). The older 4x batch solution displayed that a higher polymer concentration resulted in poorer performance. However, the most recent

4x batch displayed a clear trend where the average T_o decreased with increasing performance, which indicates that the performance increases as the polymer dose is increased. A similar concentration pattern in the different batches was also observed in the methane tests (**Table 3.2**). The trend where the KHI performance increases with higher concentrations is a widely recognized phenomenon, observed in many previous studies [28, 32, 48, 78]. A hypothesis of this phenomenon is provided by Yang et al., where they propose that a high concentration of KHI molecules leads to a saturation of the hydrate nuclei surface and thus provides a larger inhibition effect on the hydrate growth [79].

However, Lim et al. proposed a mechanism for why an increase in concentration yielded worse performance, where they explained that polymer interaction may occur at higher concentrations where a consequence of that is either that the polymers assemble into micelles or that the polymer interaction creates large and local areas of elevated concentrations. Both scenarios create a reduction in adsorption onto the hydrate surface [80].

It is currently unknown why the different batches display different behaviors regarding concentration and performance.

4.1.4 Synergist Addition Effects in SNG and Methane Systems

SNG

Synergist additions of iBGE, nBGE, DPBGE and 3 wt.% NaCl increased the performance of the PVAmBu_2O samples in SNG (**Table 3.1**).

The observed synergistic effect of iBGE and nBGE is in line with a previous study. The result from the study concluded that iBGE and nBGE in a 5000 ppm concentration provided a synergistic effect in combination with a 2500 ppm sample of PNIPMAm and that iBGE contributed to the best performance out of the two synergists [39]. A study with PVCap and the above-mentioned synergists, using the same test method, gas, and concentrations, also reached a similar conclusion where the use of iBGE obtained the best synergistic effect. PVCap alone had an average T_o of 10.4 ˚C, but following a 5000 ppm synergist addition of nBGE and iBGE, the T_o average decreased to 7.3 and 5.7 ˚C, indicating that the iBGE outperformed the nBGE. Branching was proposed as a mechanism for why iBGE had the best synergistic effect [81].

The synergism observed in the PVAmBu_2O sample with DPBGE is in agreement with results from a previous study, where DPBGE had an outstanding synergy with PVCap, as the average

onset temperature decreased to 2.0 ˚C. The increased synergistic effect is proposed to be related to additional methyl groups which give increased hydrophobicity [62].

The addition of 3 wt.% sodium chloride improved the inhibition performance of the $PVAmBu_2O$ (**Table 3.1**). This is evident as a 2.0 ˚C decrease in the average onset temperature was observed post-salt addition. Salts are a well-known class of THIs. The mechanism of hydrate inhibition in salts is that the salt ion interacts with the dipole in the water molecule [82]. The findings in **Table 3.1** are in accordance with a study performed on PVCap where the addition of 3.5 wt.% NaCl along with 0.2 wt.% $CaCl_2$ increased the KHI performance of PVCap [34].

Methane

Even though the synergist addition resulted in an increased performance in SNG, a different story was told by the methane tests (**Table 3.2**). A slight elevation (0.2 ˚C) of the average onset temperature was observed in the test containing 2500 ppm $PVAmBu_2O$ and 5000 ppm nBGE, indicating that the performance worsened with nBGE addition. A similar trend was observed with iBGE resulting in a 0.8 ˚C elevation of the average onset temperature. These findings do not correlate with previous studies, as the addition of synergists is meant to enhance the KHI performance (as discussed previously). Thus, these results can be regarded as anomalous. Although there is no available literature on why the performance deteriorated with the use of synergists, a cautious assumption may be that it is either related to the adsorption mechanism via competitive adsorption, the solubility of the synergist, or the cloud point.

The proposed competition mechanism involves that the synergist and polymer may compete for the same adsorption sites on the hydrate surface, which will lead to a decreased performance. The other reason may have to do with solubility where the glycols have not been applied close to their solubility limit. Applying a solvent near its solubility limit amplifies hydrophobic interactions with either the hydrate surface or surrounding water molecules [59]. The third reason may be linked to the polymer cloud point where the cloud point may be too high [62]. However, it is important to note that these theories are only speculations and further research would be recommended.

However, salt addition improved the performance which is in line with previous research.

4.1.5 Performance in SNG vs. Methane

The overall performance of the polyvinyl dibutyl amine oxides was better in methane than in SNG (**Figure 3.2**). This correlates well to a previous SCC test study performed with methane and SNG where the tested polymers, e.g. PVCap, displayed a lower average onset temperature in methane compared to SNG [83]. Before discussing the reasons why, there are a couple of things to consider. Firstly, methane and SNG produce different hydrate structures, namely sI, and sII, which are reported in the introductory chapter of this thesis. It is difficult to compare the performance of two different hydrate structures as sI is more symmetric compared to the more chaotic sII (**Figure 1.1**). Secondly, the SCC tests were performed with different test pressures, e.g., 76 bar for SNG and 110 bar for methane, which also impacts the performance.

The reason why the polymers seemingly performed better in methane (with respect to onset temperature values) is that each gas system produces a different subcooling at the designated test pressure. An SNG-dominated system requires a larger subcooling at T_o compared to methane [64]. This effectively means that hydrate formation occurs at a slower rate within the sII envelope leading to a higher T_o value in SNG than in methane [83]. **Appendix C**, **Figure 7.5**, provides a visual representation of each structure`s hydrate envelope. The green and purple lines are drawn for illustrational purposes. From the figure, one can see that the operational temperature at 76 bar with SNG gas is 19.5 ˚C (green line), compared to 15 ˚C for methane at 110 bar (purple line). This means that tests with SNG require a greater amount of subcooling, which serves as the driving force for hydrate formation, to initiate hydrate nucleation and subsequent growth to enable the system to enter the hydrate stability zone located on the extreme left on the phase diagram. This is why the average onset temperature is higher in SNG systems compared to methane systems.

Both of the PVAmBu_2O polymers outperformed PVCap with their designated test gases. The polymer tested with methane (**Table 3.2**) exhibited an onset temperature value as low as 2˚C, an exceptional result considering the minimum hydrate forming temperature is 2 ˚C for the SCC test. These findings indicate that the polymers could be suitable for methane systems, potentially offering superior performance. There is currently a demand in the industry for KHIs that can be utilized in methane systems as most of the commercially available KHIs are tailored for SNG systems, as sII hydrates are more thermodynamically stable and more commonly present in pipelines [72, 83]. The polymer's strong performance with both test gases (compared to PVCap) suggests that it does not exhibit a specific preference for one hydrate system over the other, indicating its potential for effective hydrate inhibition in both

systems. However, a word of caution should be added. The onset temperature values for the methane test were variable, and there were fewer tests conducted with methane compared to SNG. Therefore, conducting additional SCC tests with methane would be prudent to validate the findings.

4.1.6 Isothermal Test Results

SNG

The results from the isothermal test at 4 ˚C (**Table 3.3**) showed that the average induction time exceeded 1200 minutes when a 5000 ppm solution of $PVAmBu_2O$ was combined with 5000 ppm nBGE. The performance of this polymer and synergist blend is significantly superior to a similar study where a 2500 ppm solution of PNIPMAm (M_w= 43 000 g/mol) resulted in average an induction time of less than 120 minutes without any synergist added [60]. The approximately 18-hour difference in hydrate delay time between these samples suggests that the addition of the synergist nBGE and a two-fold concentration increase contribute to a longer hydrate delay time.

Another factor that may contribute to the increased hydrate delay time is the presence of the butyl groups and the amine oxide group. The amine oxide groups bind to the water molecules by hydrogen bonding and the butyl groups promote a better KHI effect by penetrating the hydrate cavities [60].

Adding 3 wt.% NaCl to the 4 ˚C isothermal test, which contained 5000 ppm of polymer and 5000 ppm of nBGE resulted in worse performance, as hydrates were detected at only 120 minutes. This finding contradicts the previous theories about the effect of salt addition. In addition, this result is also concerning because there is no literature available to explain it, so one should be careful not to make assumptions. However, it is worth noting that conformational changes in a KHI polymer as it adsorbs to the hydrate surface, have been reported in the past [84]. Based on that theory, a cautious assumption may be that the salt addition induced a conformational change in the polymer, making it more coiled. The coiling would have reduced the ratio between the surface area and volume, leading to a weaker interaction with the hydrate surface, and resulting in poorer performance.
As the results weren`t as good as first anticipated, the isothermal temperature was changed to 7 ˚C, as good results on VCap copolymers have been obtained with this temperature [69].

The temperature change to 7 ˚C on the 5000 ppm $PVAmBu_2O$ sample with 5000 ppm nBGE in salt yielded a surprising result. Hydrates did not form until 2192 minutes (36.5 hours), a

stark contrast to the 2500 ppm polymer sample that contained the same additions, where the average induction time was much shorter, 93 minutes. This finding suggests that a higher concentration of the polymer leads to an increased performance, as discussed previously. The 2192-minute result surpasses previous results where an induction time of 640 minutes was obtained for a copolymer of VP: VCap at 5000 ppm concentration with the same test method [69]. An additional way to verify the impressive test result is by comparing it with the sample that contained 5000 ppm PVCap with the addition of 5000 ppm nBGE where an induction time of 230 minutes (~4 hours) was achieved, which is considerably worse. These results align with previous research suggesting that the inclusion of butyl groups and nBGE as a synergist contributes to improved performance.

Unusual behavior depicting a double drop in SNG isothermal test

In the experiment (**Table 3.3**), a double pressure drop was observed in the sample containing the 2500 ppm of the new 4x batch PVAmBu$_2$O with 5000 ppm nBGE and 3 wt.% NaCl (**Figure 3.3)**. All cells exhibited a double pressure drop leading to a second t_a value after 1-3 hours. A similar double drop behavior was previously observed in a constant cooling test using 110 bar methane with 5000 ppm PNIPMAm and 5000 ppm TiPeAO. The suggested mechanism of the strange behavior was that a mixture of sI and sII hydrates emerged at a certain temperature, and a new growth period of sI hydrates initiated [64]. This may also be the case for the PVAmBu$_2$O sample, only with new growth of sII hydrates. However, since the double pressure drop was only observed in this sample and not the others, a rerun of the test would be beneficial to determine if this phenomenon was an isolated occurrence or indicative of something else.

Methane

The initial isothermal test was carried out with an isothermal temperature of 7 ˚C (**Table 3.4**), which resulted in no hydrate formation. This information implied that the hydrate formation occurred at an even lower temperature; thus, the temperature was changed to 4 ˚C.

A 51-minute induction time was observed using a mixture of 2500 ppm PVAmBu$_2$O and 5000 ppm nBGE with the addition of salt (**Table 3.4**). This performance was slightly inferior to a previous isothermal study conducted at the same pressure and temperature, using methane. In that study, a concentration of 2500 ppm of the copolymer of VP/VCap resulted in an 87-minute induction time when tested alone, and 88 minutes when tested with the addition of 5000 ppm addition nBGE [72]. Based on these comparisons, the salt addition may seem to have made the performance worse.

However, the performance of the PVAmBu_2O increased dramatically as a delay time of 735 minutes (~12 hours) was observed when the polymer concentration was increased to 5000 ppm and had the same additions of nBGE and salt. Since the salt and nBGE additions were the constant variables, it is reasonable to believe that the increased performance was only due to an increase in the polymer concentration. This is also in line with the observed trend where the performance increases as the concentration increases.

The test with 5000 ppm polymer and 5000 ppm nBGE addition had the best observable hydrate delay performance, an induction time of 1068 minutes (~18 hours). Comparing this result to the 12-hour hydrate delay time obtained with salt addition provides further evidence that salt had an antagonistic effect on the methane tests, as the hydrate delay time was decreased by six hours when salt was added. The mechanism behind the antagonistic effect of salt is cautiously explained in the section regarding isothermal test results in SNG.

Another significant discovery about this new polymer was that when combined with nBGE, it outperformed PVCap with nBGE, resulting in a 17-hour longer hydrate delay time. This further confirms the exceptional performance of this polymer.

4.2 Poly(2-dialkylamino-2-oxazoline)s

The following subchapters are dedicated to the noticeable trends and observations from the SCC tests and how they relate to previous experiments.

4.2.1 Effect of Aqueous Cell Volume on Hydrate Inhibition Performance

A cell volume of 20 mL resulted in a lower onset temperature compared to using 10 mL (**Table 3.5** and **Figure 3.4**), indicating that cell volume impacts the performance of the KHI. A higher cell volume appeared to enhance performance, while a lower volume deteriorated it. A similar conclusion was obtained in a study with Lone and Kelland [69]. The proposed explanation was related to the interface between water and gas. Decreasing the liquid volume in the cell would enhance the liquid's turbulence, causing it to cover a large portion of the cell`s steel surface. This would result in a larger interface between the gas and water, leading to a higher onset temperature at which hydrate crystals begin to form (or nucleate) on that specific plane.

4.2.2 Concentration Effects on KHI Performance in SNG and Methane

SNG

The results regarding concentration-dependent performance were similar to the PVAmBu_2O tests. Some of the polymer's performance increased with increasing concentration while others displayed that the performance decreased as the concentration increased (**Table 3.5**). Typically, it is expected that performance would improve with increasing concentration based on previous literature. However, the different structures of these polymers (**Figure 1.13**), suggest they may exhibit different performance patterns. Since these polymers are a newly discovered class, there is limited literature to compare with, aside from one study. The study briefly looked at the effects of concentration on the KHI performance with the polymer P$PyOx_{25}$, where they found that the performance increased as the polymer concentration increased [51]. Therefore, the findings in **Table 3.5** align well with the previous study regarding the increase in performance with an increase in concentration. Additionally, the trend of decreasing performance with increasing concentrations is not yet fully understood; a proposed theory is, as explained before, polymer aggregation at higher concentrations, which leads to decreased adsorption on the hydrate surface.

Methane

The findings indicated that the performance declined as the polymer concentration increased (**Table 3.6**). This is not in line with previous studies, and should therefore be investigated

further. Interestingly, the SJ258 displayed a different concentration behavior in the different test gases. In SNG, the performance increased with higher concentrations, while the opposite was observed in methane gas, as the performance deteriorated with higher concentrations. Since this was the only polymer that was tested in different concentrations in methane as well as SNG, it is challenging to assume the reason behind this variation in performance. It would be advisable to conduct further testing of the other polymers at different concentrations in methane in order to see if there is a pattern regarding this particular behavior.

4.2.3 Synergist Addition in SNG and Methane

SNG

The synergist addition of nBGE and iBGE primarily enhanced the polymer`s performance as the average onset temperature further decreased with synergist addition (**Table 3.5**). This finding is directly in line with the previously discussed theory on the synergistic effect of iBGE and nBGE. In addition, the finding is also in line with the results from the previous study where an addition of 5000 ppm iBGE to the polymer $PPyOx_{25}$ increased the polymer`s performance as a 1.9 ˚C decrease in the average T_o was observed [51].

However, the addition of iBGE to the SJ258 polymer exhibited different effects at different concentrations. At a concentration of 2500 ppm, the addition of iBGE led to synergism with the polymer, while antagonism was observed when the polymer concentration doubled to 5000 ppm. As mentioned previously, the reason behind this may be related to some sort of competition between the synergist and polymer at higher concentrations,.

The SJ192 polymer (**Table 3.5**) was tested with the synergist additions of iBGE and nBGE. A 1.4 ˚C decrease in the average T_o value was observed with 5000 ppm iBGE addition compared to a 0.8 ˚C decrease when nBGE was added. This indicates that the iBGE addition results in better performance than the nBGE addition. The results confirm the existing theory where iBGE is superior to nBGE, where the proposed reason is a branching of the molecule [81]. However, the addition of DPBGE to the SJ192 polymer yielded a 1.2 ˚C decrease in the average T_o value which is slightly poorer (0.2 ˚C) compared to the iBGE addition to the same polymer. This is also observable in **Figure 3.4**. The observed synergistic effect of DPBGE is consistent with a previous study where the DPBGE acted as a synergist for PVCap and PNIPMAm [62].

According to **Table 3.5** and **Figure 3.4**, the introduction of the synergist TiPeAO had an antagonistic effect on the performance, leading to a 2.8 ˚C increase in the average onset

temperature. This is in contrast to a previous study where the addition of 2500 ppm TiPeAO to 2500 ppm PNIPMAm resulted in complete hydrate inhibition. [64]. An assumed explanation for this effect could be aggregation between the synergist and polymer. Moreover, overdosing the SJ192 with TiPeAO and iBGE resulted in the poorest performance in the table, with a 6.0 ˚C increase in the average T_o value. KHI overdosing has been documented in the past, in a blend with PNIPMAm and TiPeAO, where the performance decreased. The suggested mechanism was aggregation between the polymer and the amine oxide [64].

The performance decreased when TiPeAB was added, as the overage onset temperature increased by approximately 3.0 ˚C. This result was unexpected, as previous reports suggested a synergistic effect with PVCap [85]. The reason for its failure to work as a synergist is not known.

The addition of 3 wt.% NaCl (**Table 3.5** and **Figure 3.5**) improved the performance of most of the polymers that were tested, which is consistent with previous results [34, 64]. However, one of the polymers, SJ272, had a 1.5 ˚C increase in the average onset temperature, which contradicts the expected trend from salt addition. Further investigations of why this occurred would be recommended.

Methane

The combined effects of iBGE in methane had unexpected results; the performance became worse when iBGE was added (**Table 3.6**). The same trend was also observed in the $PVAmBu_2O$ samples. Since this doesn`t align with what was expected, and there are no previous reports on this finding, one can only speculate the reason behind the strange results. It may be related to some sort of adsorption competition between the polymer and the synergist as explained in the discussion for the polyvinyl amine oxides. Further testing would be recommended. On the other hand, the addition of salt improved the performance, which is supported by many studies, as explained earlier.

4.2.4 Performance in SNG vs. Methane

In general, the performance of the poly(2-dialkylamino-2-oxazoline)s was similar to PVCap both in SNG and methane (**Figure 3.6**). Another trend was that the onset temperature values for the polymers in methane were approximately 2 ˚C lower than in SNG. This outcome is as expected as described earlier in the discussion for the $PVAmBu_2O$ and the same trend is also observed in a former study [83].

As previously mentioned, a low onset temperature generally indicates higher performance. Therefore, an onset temperature of 2.0 ˚C would be considered an outstanding result as this is the minimum temperature for hydrate formation in an SCC test. Given that these polymers had an approximate average onset temperature of around 10 ˚C in SNG and 8 ˚C in methane, it can be inferred that the performance of these new polymers was generally good (compared to PVCap) in both systems, but not outstanding as the onset temperature did not reach a value as low as 2 ˚C.

An explanation of why the performance seems to be better in methane than SNG is provided earlier in the discussion. The reason is related to the different subcooling in each system.

5 Conclusion and Further Work

This chapter contains a summary and conclusion of the important findings with both chemical groups and a proposal for further work.

5.1 Conclusion

This thesis aimed to design and test the performance of two new classes of kinetic hydrate inhibitors (KHIs), namely polyvinyl amine oxides and poly(2-dialkylamino-2-oxazoline)s. The performance test method was the constant cooling method. Both polymers were tested in SNG at 76 bar and methane at 110 bar. Additionally, isothermal tests were conducted on the polyvinyl amine oxides to further explore their performance as KHIs. The polyvinyl amine oxides were a brand new class of KHIs that had never been synthesized or tested in the laboratory before. The reason for why it was designed, was to try and meet the industry need for an easy synthesizable KHI that can be available in large quantities. The poly(2-dialkylamino-2-oxazolines) were polymers obtained through collaboration with UiS and the Hoogenboom research group in Belgium. Further investigation of the KHI performance of the poly(2-dialkylamino-2-oxazoline)s was conducted as only a small study had been previously performed.

5.1.1 Synthesis of the Polyvinyl Amine Oxides

The results of the constant cooling test for the various syntheses of the polyvinyl amine oxides indicated that the bromo alkane alternatives, particularly the di-butylated variants ($PVAmBu_2O$), exhibited the best performance. A surprising result was that the pentylated version did not work as it was not soluble in water.

The substitution of isobutyronitrile with acetonitrile resulted in decreased performance, possibly due to their different water solubilities, which may affect reaction kinetics and chemical availability.

The synthesized $PVAmBu_3Br$ performed poorly, as confirmed by the NMR spectrum. These results indicate the importance of the presence of an amine oxide group for good KHI performance.

The synthesis of the polyvinyl dibutyl amine oxides had a significant drawback: it did not consistently yield the same product, as evidenced by the varying average onset temperature

values in the constant cooling tests at the same test concentration (2500 ppm). This inconsistency underlines the need to refine the synthesis process to ensure reproducibility.

5.1.2 Slow Constant Cooling Test for Polyvinyl Amine Oxides

Firstly, the slow constant cooling test showed that most of the polyvinyl amine oxides functioned as KHIs as their performance outcompeted that of deionized water. Secondly, the low molecular weight $PVAmBu_2O$ produced the best performance. However, the performance of the low molecular weight alternative was not better than PVCap. In addition, there was not a clear pattern between concentration and performance as some samples displayed a trend of increasing performance with increasing polymer concentrations, while others did not.

The addition of the synergists iBGE, nBGE,DPBGE and 3 wt.% NaCl in synthetic natural gas (SNG) improved the KHI performance as the average onset temperature values decreased. However, the methane tests yielded unexpected results, as the synergist additions of iBGE and nBGE seemed to make the performance worse. Possible reasons for this unexpected outcome include adsorption competition between the synergist and KHI molecules or factors related to the solubility of the synergist or the cloud point.

The $PVAmBu_2O$ polymers with low molecular weight outperformed the commercial product PVCap in SNG and methane. However, the result in SNG was in contrast to a previous result with one of the first $PVAmBu_2O$ syntheses as it did not outperform PVCap. These results indicate the need for refinement in the synthesis process to yield trustworthy results. Furthermore, the polymer appeared to be compatible with both sI and sII systems. The onset temperature in the methane tests reached as low as 2 ˚C indicating that these polymers are most effective in sI systems. Further studies on methane systems are recommended to assess the methane system compatibility and may also fulfill a need in the KHI industry where there is a need for KHIs suitable for methane systems.

5.1.3 Isothermal Test for Polyvinyl Amine Oxides

Isothermal tests using SNG at 4 ˚C resulted in an induction time of over 1200 minutes with the combination of 5000 ppm $PVAmBu_2O$ with 5000 ppm nBGE. In contrast, the same chemical blend had an induction time of 2192 minutes when the isothermal temperature was changed to 7 ˚C. This was considerably better than PVCap and nBGE at a 5000+5000 ppm concentration, which had an induction time of 230 minutes. However, the addition of 3 wt.% NaCl resulted in worse performance.

An unusual double pressure drop behavior was discovered in the sample containing 2500 ppm $PVAmBu_2O$ and 5000 ppm nBGE with salt. The behavior may be related to the formation of sI and sII hydrates. Additional testing would be recommended.

The 7 ˚C methane isothermal tests yielded an induction time of 1068 minutes with the sample containing 5000 ppm $PVAmBu_2O$ and 5000 ppm nBGE. Compared to PVCap and nBGE at equivalent concentrations, the $PVAmBu_2O$ polymer and synergist addition exhibited a 17-hour longer hydrate delay time, indicating excellent performance. The trend of increasing performance due to increased concentrations was also observed. However, the addition of 3 wt.% NaCl resulted in decreased performance as the average induction time increased by six hours. Polymer coiling as a result of salt addition has been proposed as a possible explanation.

5.1.4 Slow Constant Cooling Test for Poly(2-dialkylamino-2-oxazoline)s

Aqueous cell volume impacted the performance of the polymers, where a 20 mL cell volume resulted in a better performance than 10 mL.

In SNG, some of the polymers displayed the classic trend of increasing performance with increasing concentrations, while others displayed a decrease in performance with increasing concentrations. Additionally, for the methane tests, the polymer performance became worse with increasing concentrations.

Synergist additions in SNG revealed that additions of iBGE, nBGE, and DPBGE increased the KHI performance of the polymers. However, overdosing the polymer with 2500 ppm TiPeAO and 10 000 ppm iBGE resulted in the worst performance as the average onset temperature was increased by 6 ˚C. Additionally, the TiPeAO and TiPeAB additions made the performance worse. The addition of 3 wt.% NaCl generally increased the performance, as expected. However, the methane tests revealed that iBGE additions provided an antagonistic effect on the average onset temperature. This has not been observed previously and it would be recommended to do further testing with other polymers and to try and understand the mechanism for why this happened.

The performance in both tes gas systems, SNG and methane, was similar to PVCap. This indicates that the polymers are not sI and sII specific and may be used in both systems.

5.2 Further Work

A possible extension of this study is to combine the KHIs with THIs to examine their combined performance. The addition of THIs could potentially enhance the inhibitory effect of the KHI. However, A CGI study performed in methane concluded that the additions of methanol and ethanol to PVCap deteriorated the performance of PVCap. This was attributed to the fact that methanol and ethanol are also hydrate-forming agents, which would cause a competition where the amide group on PVCap competes with the hydrates formed from methanol and ethanol to enclathrate the open cages of the hydrate structure. On the other hand, the combined effect of the THI and the KHI was still better than using the THI alone. Additionally, MEG was shown to serve as a top-up inhibitor for PVCap [86]. According to Semenov et. Al, MEG has also been demonstrated to work well with the VP: VPCap copolymer in a methane system [87].

Another alternative is to investigate NaCl addition with higher weight percentages (e.g. 5%, 10%, and 15%). This has already been performed by Ghosh et al. with PNIPMAm in various concentrations where the best effect was in the sample containing 1000 ppm PNIPMAm and 15 wt.% NaCl as an onset temperature below 2 ˚C was achieved [64].The performance testing in different salinity brines is imperative as the formation water contains substantial salinity and the KHI has a tendency to precipitate under such conditions due to its limited solubility [88]. The limited polymer solubility is due to a significant decrease in the cloud point under high aqueous salinity conditions, resulting in less miscibility in the water phase [89].

A third alternative could be to increase the KHI bioavailability and performance by introducing proteins as synergists. Bovine serum albumin and peptone have displayed synergism with PVP and PVCap [90]. However, the induction times were not as long as for the traditional chemical synergists explored in this thesis. To mitigate this problem, a proposal may be to combine the KHI polymer with the traditional chemical synergist and protein synergist to see if the KHI performance is enhanced.

6 References

1. Bai Y, Bai Q. 1.1 Introduction. In: Bai Y, Bai Q, editors. Subsea Engineering Handbook. Boston, MA: Gulf Professional Publishing; 2010. p. 3-6.

2. Lee W, Shin J-Y, Kim K-S, Kang S-P. Synergetic Effect of Ionic Liquids on the Kinetic Inhibition Performance of Poly(N-vinylcaprolactam) for Natural Gas Hydrate Formation. Energy Fuels. 2016;30(11):9162-9.

3. Tohidi B, Anderson R, Mozaffar H, Tohidi F. The Return of Kinetic Hydrate Inhibitors. Energy Fuels. 2015;29(12):8254-60.

4. Bai Y, Bai Q. Chapter 12 - Subsea System Engineering. In: Bai Y, Bai Q, editors. Subsea Engineering Handbook. Boston: Gulf Professional Publishing; 2010. p. 331-47.

5. Gauls D. Gas hydrates: importance and applications in petroleum exploration. Marine and Petroleum Geology. 2001;18(4):519-23.

6. Bai Y, Bai Q. Chapter 15 - Hydrates. In: Bai Y, Bai Q, editors. Subsea Engineering Handbook. Boston, MA: Gulf Professional Publishing; 2010. p. 451-81.

7. Mokhatab S, Wilkens RJ, Leontaritis KJ. A Review of Strategies for Solving Gas-Hydrate Problems in Subsea Pipelines. Energy Sources, Part A: Recovery, Utilization, and Environmental Effects 2007;29(1):39-45.

8. Sloan ED, Koh CA. Clathrate Hydrates of Natural Gases. Third ed. Boca Raton, Florida: CRC Press (Taylor & Francis group); 2008.

9. Joshi SV, Grasso GA, Lafond PG, Rao I, Webb E, E. Zerpa L, et al. Experimental flowloop investigations of gas hydrate formation in high water cut systems. Chemical Engineering Science. 2013;97:198-209.

10. Koh CA, Westacott RE, Zhang W, Hirachand K, Creek JL, Soper AK. Mechanisms of gas hydrate formation and inhibition. Fluid Phase Equilibria. 2002;194-197:143-51.

11. Hassanpouryouzband A, Joonaki E, Farahani MV, Takeya S, Ruppel C, Yang J, et al. Gas hydrates in sustainable chemistry. Chemical Society Reviews. 2020;49:5525-309.

12. Wei W-N, Li B, Gan Q, Li Y-L. Research progress of natural gas hydrate explotation with CO2 replacement: A review. Fuel. 2022;312.

13. V.Joshi S, Grasso GA, G.Lafond P, Rao I, Webb E, Zerpa LE, et al. Experimental flowloop investigations of gas hydrate formation in high water cut systems. Chemical Engineering Science [Internet]. 2013 9th of October 2023; 97:[198-209 pp.].

14. Luna-Ortiz E, Healey M, Anderson R, Sørhaug E. Crystal Growth Inhibition Studies for the Qualification of a Kinetic Hydrate Inhibitor under Flowing and Shut-In Conditions. Energy Fuels. 2014;28(5):2902-13.

15. Khurana M, Yin Z, Linga P. A Review of Clathrate Hydrate Nucleation. ACS Sustainable Chem Eng. 2017;5(12):11176-203.

16. Ellison BT, Gallagher CT, Frostman LM, Lorimer SE. The Physical Chemistry of Wax, Hydrates, and Asphaltene. Offshore Technology Conference; Houston Texas: OTC; 2000.

17. Kelland MA. Production chemicals for the oil and gas industry: CRC Press 2014.

18. Sum AK, Koh CA, Sloan ED. Developing a Comprehensive Understanding and Model of Hydrate in Multiphase Flow: From Laboratory Measurements to Field Applications. Energy Fuels. 2012;26(7):4046-52.

19. Hussein A. Chapter 16 - Essentials of Flow Assurance Solids in Oil and Gas Operations Understanding Fundamentals, Characterization, Prediction, Environmental Safety and Management 2022.

20. Duchateau C, Glénat P, Pou T-E, Hidalgo M, Dicharry C. Hydrate Precursor Test Method for the Laboratory Evaluation of Kinetic Hydrate Inhibitors. Energy Fuels. 2010;24:616-23.

21. Tabaaza GA, Haq IU, Zain DB, La B. Toxicological issues of conventional gas hydrate inhibitors. Process safety progress. 2021;41(S1):S135-S40.

22. A. Kaviraj, Bhunia F, Saha NC. Toxicity of Methanol to Fish, Crustacean, OligochaeteWorm, and Aquatic Ecosystem. International Jorunal of Toxicology.23(1):55-63.

23. Kelland MA. History of the Development of Low Dosage Hydrate Inhibitors. Energy Fuels 2006;20(3):825-47.

24. Ke W, Chen D. A short review on natural gas hydrate, kinetic hydrate inhibitors and inhibitor synergists. Chinese Journal of Chemical Engineering. 2019;27:2049-61.

25. Kelland MA, Svartaas TM, Øvsthus J, Namba T. A New Class of Kinetic Hydrate inhibitor. Annals of the New York Academy of Sciences. 2006;912(1):281-93.

26. Reza J, Trejo A, Rebolledo-Libreros ME, Guzmán-Lucero D. Inhibition of structure II hydrates formation by salt-tolerant N-vinyl lactam-based terpolymers. Journal of Natural Gas Science and Engineering. 2018;56:175-92.

27. Singh A, Suri A. Synergistic Kinetic Hydrate Inhibition of Pectin, PVP, and PVCap with Monoethylene Glycol. Energy Fuels. 2023;37(6):4524-43.

28. Reyes FT, Kelland MA. First Investigation of the Kinetic Hydrate Inhibitor Performance of Polymers of Alkylated N-Vinyl Pyrrolidones. Energy Fuels. 2013;27(7):3730-5.

29. Walker VK, Zeng H, Ohno H, Daraboina N, Sharifi H, Bagherzadeh SA, et al. Antifreeze proteins as gas hydrate inhibitors. Canadian Journal of Chemistry. 2015;93(8):839-49.

30. Kamal MS, Hussein IA, Sultan AS, Solms Nv. Application of various water soluble polymers in gas hydrate inhibition. Renewable and Sustainable Energy Reviews. 2016;60:206-25.

31. Dirdal EG, Kelland MA. Does the Cloud Point Temperature of a Polymer Correlate with Its Kinetic Hydrate Inhibitor Performance? Energy Fuels. 2019;33(8):7127-37.

32. Zhang Q, Kelland MA, Frey H, Blankenburg J, Limmer L. Amine N-Oxide Kinetic Hydrate Inhibitor Polymers for High-Salinity Applications. Energy Fuels. 2020;34(5):6298-305.

33. Qian Zhang, Shen X, Zhou X, Liang D. Inhibition Effect Study of Carboxyl-Terminated Polyvinyl Caprolactam on Methane Hydrate Formation. Energy Fuels. 2017;31(1):839-46.

34. Dirdal EG, A.Kelland M. Further Investigation of Solvent Synergists for Improved Performance of Poly(N-vinylcaprolactam)-Based Kinetic Hydrate Inhibitors. Energy Fuels. 2021;35(24):20103-16.

35. Chua PC, Kelland M. Poly(N-vinyl azacyclooctanone): A More Powerful Structure II Kinetic Hydrate Inhibitor than Poly(N-vinyl caprolactam). Energy Fuels. 2012;26(7):4481-5.

36. Liu J, Wang H, Guo J, Chen G, Zhong J, Yan Y, Zhang J. Molecular insights into the kinetic hydrate inhibition performance of Poly(N-vinyl lactam) polymers Journal of Natural Gas Science and Engineering. 2020;83.

37. Chua PC, Kelland MA, Ishitake K, Satoh K, Kamigaito M, Okamoto Y. Kinetic Hydrate Inhibition of Poly(N-isopropylmethacrylamide)s with Different Tacticities. Energy Fuels. 2012;26(6):3577-85.

38. Chua PC, Kelland MA, Hirano T, Yamamoto H. Kinetic Hydrate Inhibition of Poly(N-isopropylacrylamide)s with Different Tacticities. Energy Fuels. 2012;26(8):4961-7.

39. Ree LHS, Kelland MA. Investigation of Solvent Synergists for Improved Kinetic Hydrate Inhibitor Performance of Poly(N-isopropyl methacrylamide). Energy Fuels. 2019;33(9):8231-40.

40. Ree LHS, Opsahl E, Kelland MA. N-Alkyl Methacrylamide Polymers as High Performing Kinetic Hydrate Inhibitors. Energy Fuels. 2019;33(5):4190-201.

41. Kelland MA. Tailored Amine Oxides─Synergists, Surfactants, and Polymers for Gas Hydrate Management, a Minireview. Energy Fuels. 2023;37(13):8919-34.

42. Singh SK, Bajpai M, Tyagi VK. Amine Oxides: A Review. Journal Oleo Science. 2006;55(3):99-119.

43. Goracci L, Germani R, Rathman JF, Savelli G. Anomalous Behavior of Amine Oxide Surfactants at the Air/Water Interface. Langmuir. 2007;23:10525-32.

44. Kelland MA, Kvæstad AH, Astad EL. Tetrahydrofuran Hydrate Crystal Growth Inhibition by Trialkylamine Oxides and Synergism with the Gas Kinetic Hydrate Inhibitor Poly(N-vinyl caprolactam). Energy Fuels. 2012;26(7):4454-64.

45. Kelland MA, Pomipic J, Ghosh R, Abdel-Azeim S. N-Vinyl Caprolactam/Maleic-Based Copolymers as Kinetic Hydrate Inhibitors: The Effect of Internal Hydrogen Bonding. Energy Fuels. 2022;36(6):3088-96.

46. Kelland MA, Mady MF. Acylamide and Amine Oxide Derivatives of Linear and Hyperbranched Polyethylenimines. Part 1: Comparison of Tetrahydrofuran Hydrate Crystal Growth Inhibition Performance. Energy Fuels. 2016;30(5):3934-40.

47. Zhang Q, Kelland MA, Lu H. Non-amide kinetic hydrate inhibitors: A review Fuel. 2022;315.

48. Zhang Q, Limmer L, Frey H, Kelland MA. N-Oxide Polyethers as Kinetic Hydrate Inhibitors: Side Chain Ring Size Makes the Difference. Energy & Fuels. 2021;35(5):4067-74.

49. Jana S, Hoogenboom R. Poly(2-oxazoline)s: a comprehensive overview of polymer structures and their physical properties—an update. Polymer International. 2022;71(8):935-49.

50. Villano LD, Kommedal R, Fijten MWM, Schubert US, Hoogenboom R, Kelland MA. A Study of the Kinetic Hydrate Inhibitor Performance and Seawater Biodegradability of a Series of Poly(2-alkyl-2-oxazoline)s. Energy Fuels. 2009;23:3665-73.

51. Kelland MA, Jana S, Pomipic J, Sedlacek O, Hoogenboom R. Kinetic Hydrate Inhibition from Thermoresponsive Poly(2-amino-2-oxazoline)s: Size and Shape of the Hydrophobic Groups Are Critical for Performance. Energy Fuels. 2024;38(5):3784-91.

52. Yagasaki T, Matsumoto M, Tanaka H. Adsorption of Kinetic Hydrate Inhibitors on Growing Surfaces: A Molecular Dynamics Study. Journal of Physical Chemistry. 2018;122:3396-406.

53. Zhang JS, Lo C, Couzis A, Somasundaran P, Wu J, Lee JW. Adsorption of Kinetic inhibitors on Clathrate Hydrates. Journal of Physical Chemistry. 2009;113:17418-20.

54. Zhi Li FJ, Qin H, Liu B, Sun C, Chen G. Molecular dynamics method to simulate the process of hydrate growth in the presence/absence of KHIs. Chemical Engineering Science. 2017;164:307-12.

55. Mozaffar H, Anderson R, Tohidi B. Reliable and Repeatable Evaluation of Kinetic Hydrate Inhibitors Using a Method Based on Crystal Growth Inhibition. Energy Fuels. 2016;30(12):10055-63.

56. Zeng H, Wilson LD, Walker VK, Ripmeester JA. Effect of Antifreeze Proteins on the Nucleation, Growth, andthe Memory Effect during Tetrahydrofuran Clathrate HydrateFormation. Journal of the American Chemical Society. 2006;128(9):2760-3106.

57. Zhang S-w, Shang L-y, Binama M, Lv Z, Liu Z, Sun X, Wang J. Inhibition of N-vinylpyrrolidone on hydrate in high-pressure flow system under the synergistic effect of ether compounds. Journal of Molecular Liquids. 2022;367.

58. Zou X, Zi M, Wu T, Yao Y, Yang C, Chen D. Synthesis and evaluation investigation of novel kinetic hydrate inhibitors at high subcooling conditions Fuel. 2023;341(1).

59. Kelland MA, Dirdal EG. Powerful Synergy of Acetylenic Diol Surfactants with Kinetic Hydrate Inhibitor Polymers—Choosing the Correct Synergist Aqueous Solubility. Energy Fuels. 2021;35(19):15721-7.

60. Ghosh R, Kelland MA. Pushing the Known Performance Envelope of Kinetic Hydrate Inhibitors─Powerful Synergy of Trialkylamine Oxides with Acrylamide-based Polymers. Energy Fuels. 2022;36(1):341-9.

61. Huang X, Zhu R, Cheng L, Zhu Y, Xiao P, Wang X, et al. Synthesis and evaluation of poly (N-vinyl caprolactam)–co-tert-butyl acrylate as kinetic hydrate inhibitor. Chinese Journal of Chemical Engineering. 2022;50:317-25.

62. Kelland MA, Dirdal EG, Pomipic J, Ajiro H, Nag A. Kinetic Hydrate Inhibitors: The Effect of Pre- or Postpolymerization Solvent Addition on Performance and a Powerful New Glycol Ether Solvent Synergist. Energy Fuels. 2023;37(16):11853-63.

63. Kelland MA, Dirdal EG, Ree LHS. Solvent Synergists for Improved Kinetic Hydrate Inhibitor Performance of Poly(N-vinylcaprolactam). Energy Fuels. 2020;34(2):1653-63.

64. Ghosh R, Pomicpic J, Kelland MA. High-Performance Kinetic Hydrate Inhibition with Poly(N-isopropyl methacrylamide) and Triisopentylamine Oxide─Surprising Concentration-Dependent Results. Energy Fuels. 2023;37(7):4928-36.

65. Kelland M. Polyamine Oxides (PAOs) as Kinetic Hydrate Inhibitors for Gas and Oil Flow Assurance. JIRP Webinar; 2021. p. https://www.youtube.com/watch?v=1x9SAsjFV8&t=146s.

66. Kelland MA, Dirdal EG, Zhang Q. High Cloud Point Polyvinylaminals as Non-Amide-Based Kinetic Gas Hydrate Inhibitors. Energy Fuels. 2020;34:8301-7.

67. Germany PS. Examine Gas Hydrate Formation with the Rocking Cell RC5. Germany: PSL Systemtechnik GmbH; 2015.

68. Anderson R, H.Mozaffar, K.Tohidi. Development of a Crystal Growth Inhibition Based Method for the Evaluation of Kinetic Hydrate Inhibitors. Proceedings of the 7th International Conference on Gas Hydrates (ICGH 2011); Edinburgh, United Kingdom2011. p. 2161-74.

69. Lone A, A. Kelland M. Exploring Kinetic Hydrate Inhibitor Test Methods and Conditions Using a Multicell Steel Rocker Rig. Energy Fuels. 2013;27(5):2536-47.

70. Villano LD, Kelland MA. An investigation into the laboratory method for the evaluation of the performance of kinetic hydrate inhibitors using superheated gas hydrates. Chemical Engineering Science. 2011;66:1973-85.

71. Kelland M. Preparation of the PVCap powder used for testing. In: Kiær J, editor. 2024.

72. Zhang Q, Kelland MA. Kinetic inhibition performance of alkylated polyamine oxides on structure I methane hydrate. Chemical Engineering Science. 2020;220.

73. ACS. Molecule of the week archive Acetonitrile: American Chemical Society; 2013 [Available from: https://www-acs-org.ezproxy.uis.no/molecule-of-the-week/archive/a/acetonitrile.html.

74. ACS. Molecule of the week archive Isobutyronitrile: American chemical society; 2021 [Available from: https://www-acs-org.ezproxy.uis.no/molecule-of-the-week/archive/i/isobutyronitrile.html.

75. Ahmadi M, Seyedin SH. Investigation of NaOH Properties, Production and Sale Mark in the world. Journal of Multidisciplinary Engineering Science and Technology 2019;6(10).

76. Chua PC, Kelland MA, Ajiro H, Sugihara F, Akashi M. Poly(vinylalkanamide)s as Kinetic Hydrate Inhibitors: Comparison of Poly(N-vinylisobutyramide) with Poly(N-isopropylacrylamide). Energy Fuels. 2013;27(1):183-8.

77. O'Reilly R, Ieong NS, Chua PC, Kelland MA. Missing Poly(N-vinyl lactam) Kinetic Hydrate Inhibitor: High-Pressure Kinetic Hydrate Inhibition of Structure II Gas Hydrates with Poly(N-vinyl piperidone) and Other Poly(N-vinyl lactam) Homopolymers. Energy Fuels. 2011;25(10):4595-9.

78. Zhang Q, Heyns IM, Pfukwa R, Klumperman B, Kelland MA. Improving the Kinetic Hydrate Inhibition Performance of 3-Methylene-2-pyrrolidone Polymers by N-Alkylation, Ring Expansion, and Copolymerization. Energy Fuels. 2018;32(12):12337-44.

79. Yang C, Zi M, Wu G, Zou X, Liu K, Chen D. Concentration effect of kinetic hydrate inhibitor on hydrate formation and inhibition Fuel. 2022;323.

80. Lim VWS, Metaxas PJ, Johns ML, Haandrikman G, Crosby D, Aman ZM, May EF. The delay of gas hydrate formation by kinetic inhibitors. Chemical Engineering Journal. 2021;411.

81. Kelland MA, Dirdal EG, Ree LHS. Solvent Synergists for Improved Kinetic Hydrate Inhibitor Performance of Poly(N-vinylcaprolactam). Energy Fuels. 2020;34(2):1653-63.

82. Semenov AP, Stoporev AS, Mendgaziev RI, Gushchin PA, Khlebnikov VN, Yakushev VS, et al. Synergistic effect of salts and methanol in thermodynamic inhibition of sII gas hydrates. The Journal of Chemical Thermodynamics. 2019;137:119-30.

83. Abrahamsen E, Kelland MA. Comparison of Kinetic Hydrate Inhibitor Performance on Structure I and Structure II Hydrate-Forming Gases for a Range of Polymer Classes. Energy Fuels. 2018;32(1):342-51.

84. Perrin A, Goodwin MJ, Musa OM, Berry DJ, Orcid PC, Edkins K, et al. Hydration Behavior of Polylactam Clathrate Hydrate Inhibitors and Their Small-Molecule Model Compounds. Crystal, Growth & Design. 2017;17(6):3236-49.

85. Chua PC, Kelland MA. Tetra(iso-hexyl)ammonium Bromide—The Most Powerful Quaternary Ammonium-Based Tetrahydrofuran Crystal Growth Inhibitor and Synergist with Polyvinylcaprolactam Kinetic Gas Hydrate Inhibitor. Energy Fuels. 2012;26(2):1160-8.

86. Mozaffar H, Anderson R, Tohidi B. Effect of alcohols and diols on PVCap-induced hydrate crystal growth patterns in methane systems. Fluid Phase Equilibria. 2016;425:1-8.

87. Semenov AP, Gong Y, Medvedev VI, Stoporev AS, Istomin VA, Vinokurov VA, Li T. New insights into methane hydrate inhibition with blends of vinyl lactam polymer and methanol, monoethylene glycol, or diethylene glycol as hybrid inhibitors. Chemical Engineering Science. 2023;268.

88. Webber P, Morales N, Madden A. Development and Implementation of a High Temperature and Salinity Tolerant Kinetic Hydrate Inhibitor to Replace an Existing, Ten-Year Continuous Application. Offshore Technology Conference; Houston, Texas: Offshore Technology Conference; 2014. p. 8.

89. Tohidi F, Anderson R, Tohidi B. Evaluation of a Novel Water-Immiscible Kinetic Hydrate Inhibitor Formulation. Energy Fuels. 2018;32(6):6518-23.

90. Singh A, Suri A. Enhanced Hydrate Inhibition Using Protein Synergists with Kinetic Hydrate Inhibitors. Energy Fuels. 2022;36(17):10395-404.

7 Appendices

Appendix A. NMR results of $PVAmBu_3Br$

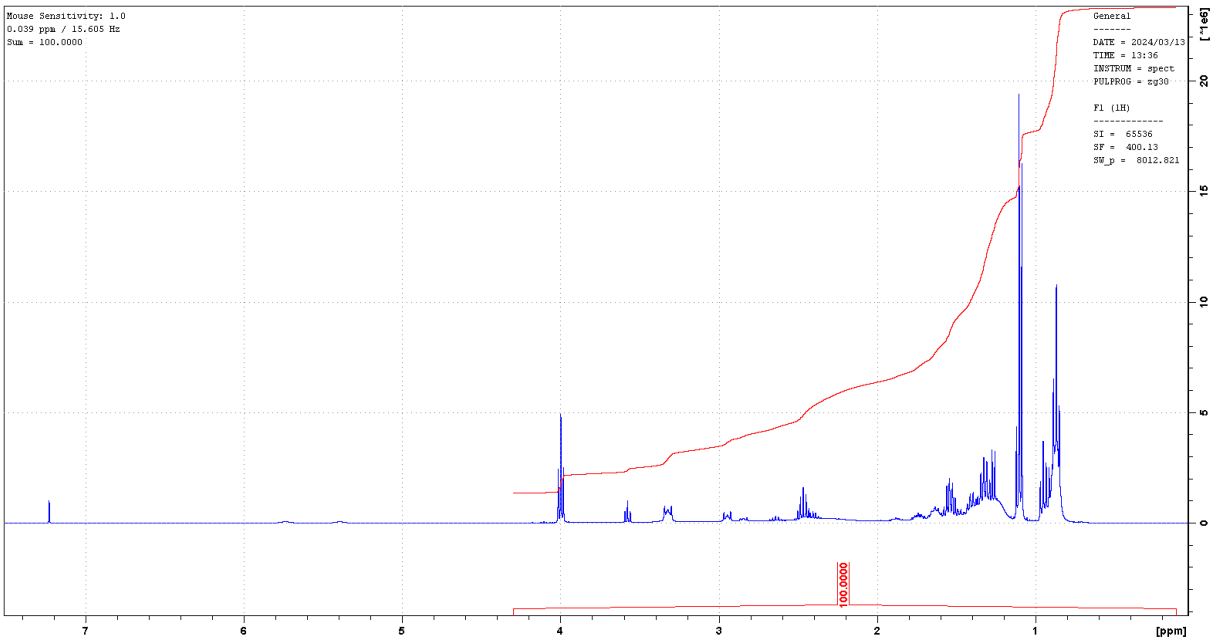

Figure 7.1 *^1H NMR spectrum of $PVAmBu_3Br$ in $CDCl_3$.*

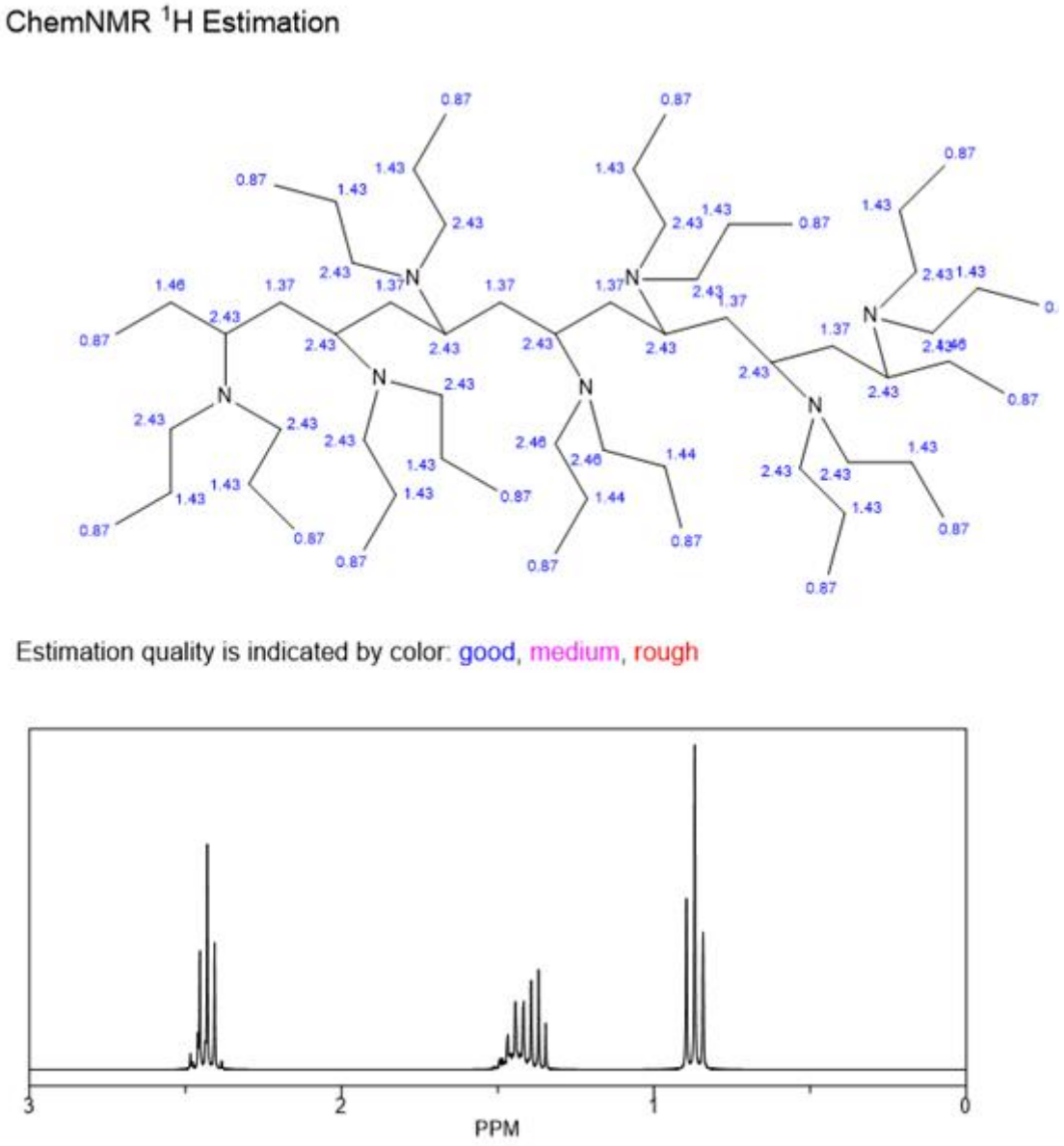

Figure 7.2 *ChemDraw prediction NMR spectrum PVAmBu₃Br.*

Appendix B. NMR results of $PVAmBu_2$

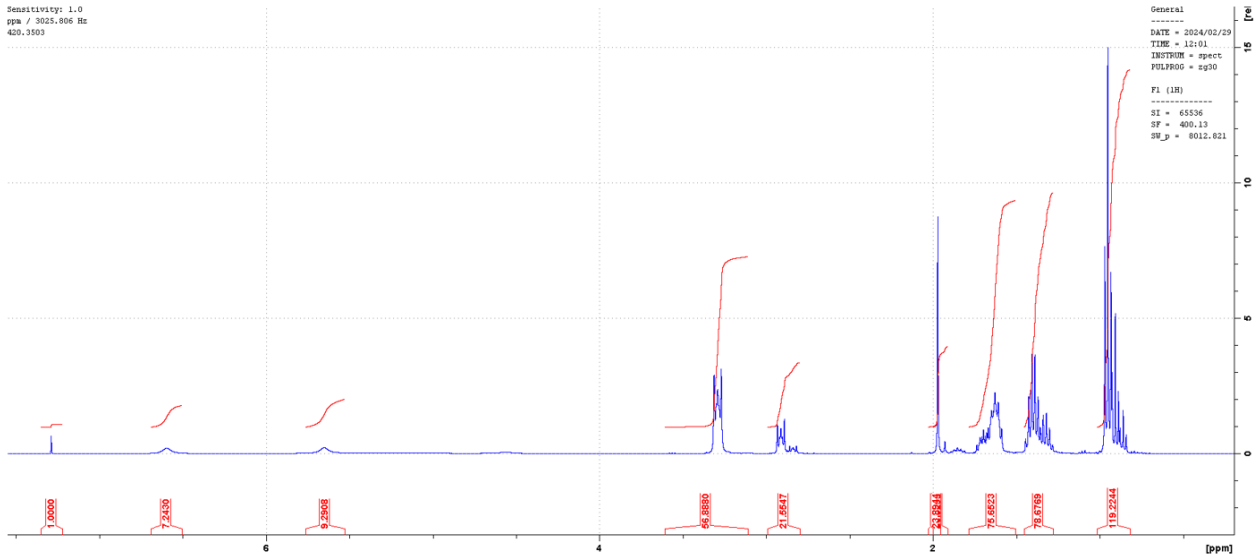

Figure 7.3 *^1H NMR spectrum of $PVAmBu_2$ in DMSO.*

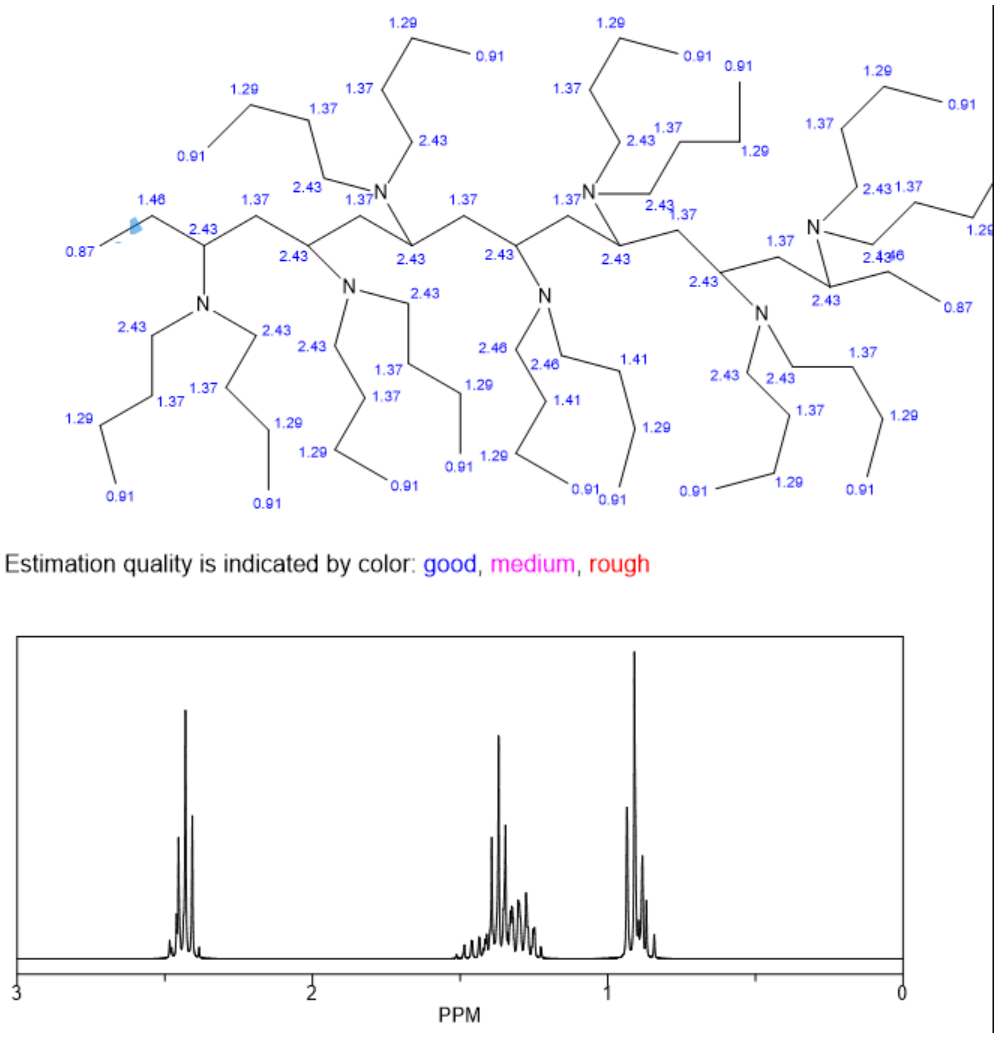

Figure 7.4 *ChemDraw prediction of PVAmBu₂ in DMSO.*

Appendix C. Hydrate Formation Envelope and Subcooling in SNG and Methane

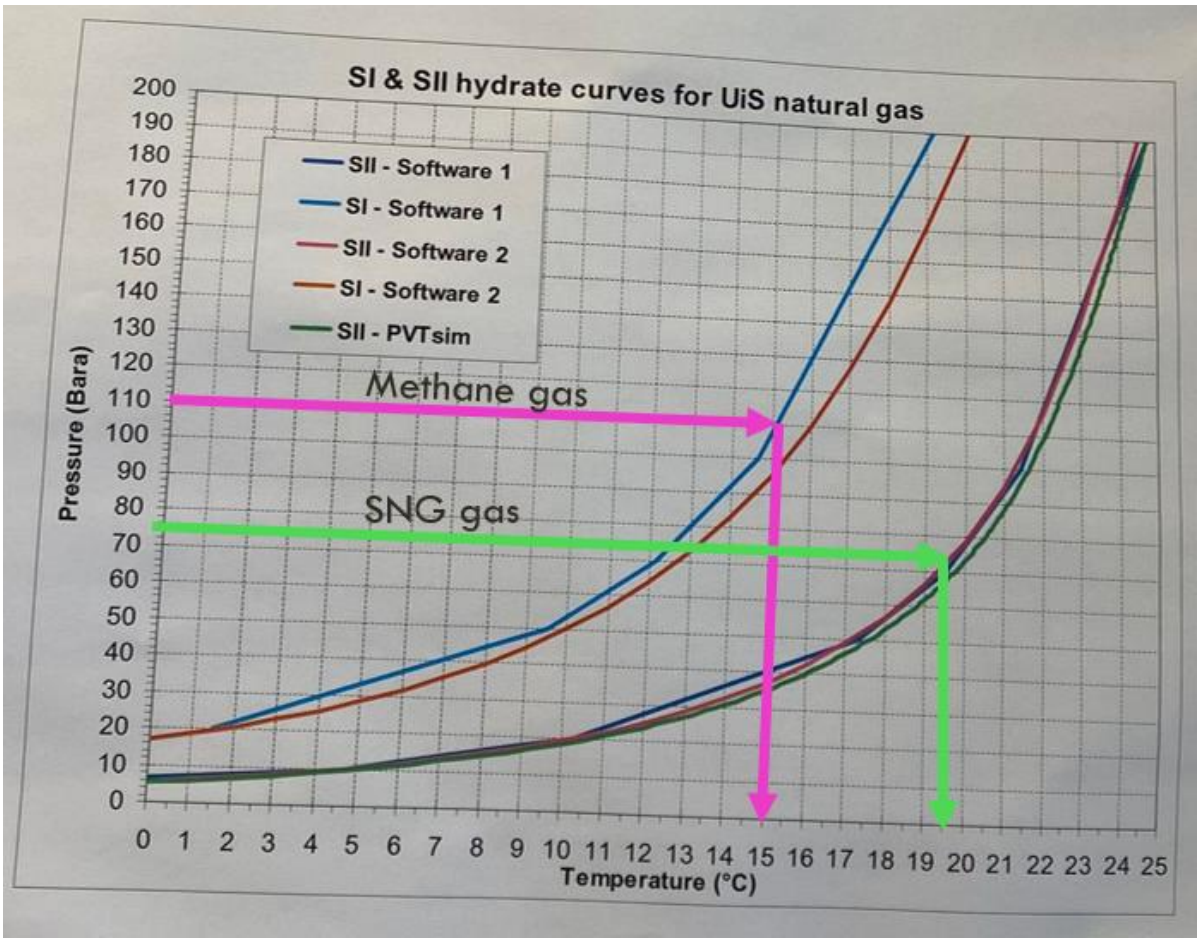

Figure 7.5 Hydrate envelope for sI and sII hydrates in SNG and methane. The figure is retrieved from the RC5-2 lab at UiS.